THESIS

ECTOPIC EXPRESSION OF R2R3-MYB TRANSCRIPTION FACTORS TO CONTROL

SUBERIN BIOSYNTHESIS

Submitted by

Nick Berning

Department of Biology

In partial fulfillment of the requirements

For the Degree of Master of Science

Colorado State University

Fort Collins, Colorado

Summer 2022

Master's Committee:

      Advisor: June Medford

      Christie Peebles
      Dan Sloan

ABSTRACT

ECTOPIC EXPRESSION OF R2R3-MYB TRANSCRIPTION FACTORS TO CONTROL

SUBERIN BIOSYNTHESIS

Minimizing the deleterious effects of abiotic stresses on cultivated plants is critical to maximizing crop yield. Suberin is a glycerol based polyester found in the endodermis, seed coat, cork cells, and areas of wounding in the epidermis. Recently, suberin biosynthesis has been shown to be at least partially regulated by a set of R2R3-MYB transcription factors.

The ability to control suberin biosynthesis in specific plant tissues could be a valuable biotechnological tool in designing plants which can withstand higher degrees of abiotic stress. In this thesis, I detail a genetic screen of four different R2R3-MYB transcription factor's ability to induce ectopic suberin formation in the root epidermis of *Arabidopsis thaliana*. Subsequently, I characterize the transcription factor with the greatest ability to induce ectopic suberin biosynthesis, MYB92.

MYB92, when expressed in the root epidermis, consistently forms a suberin barrier within that tissue. Plants expressing MYB92 in the root epidermis may be stunted and chlorotic under typical growth conditions, however, they outperform wild-type Col-0 plants under salt stress. More characterization of ectopic, suberin barrier's ability to confer salt tolerance could be performed in order to understand how epidermal suberin might perform in crop plants.

TABLE OF CONTENTS

Chapter One: Introduction

1.1 Plant barriers and suberin lamellae

Physical barriers are essential to all organisms to separate the internal components of the organism from the extracellular or extra-organismal environment. In sessile organisms, such as plants, the ability of barriers to respond to the environment is crucial to their survival. Because plants cannot move during dynamic environmental conditions, they must often adapt to the conditions they are currently experiencing. The primary barrier in the above-ground plant organs is the cuticle, a protective coating composed mainly of cutin impregnated by cuticular waxes. Within the plant root is a barrier known as the endodermis. The root endodermis defines a line between the soil and the root by controlling access to the root stele, and thus the rest of the plant. It functions to both reduce water and ion loss from the stele and keep pathogens and toxic ions out of the stele. The endodermis is a ring of cells between the stele and surrounding root cortex that provides apoplast and transcellular barriers, in the form of the lignified Casparian strips and suberized lamellae respectively (fig. 1.1) (Bonnett 1968; Singh and Jacobson 1977; Moon et al. 1986; Aloni et al. 1998; Cholewa 2000, Alassimone et al. 2010; Barberon et al. 2016).
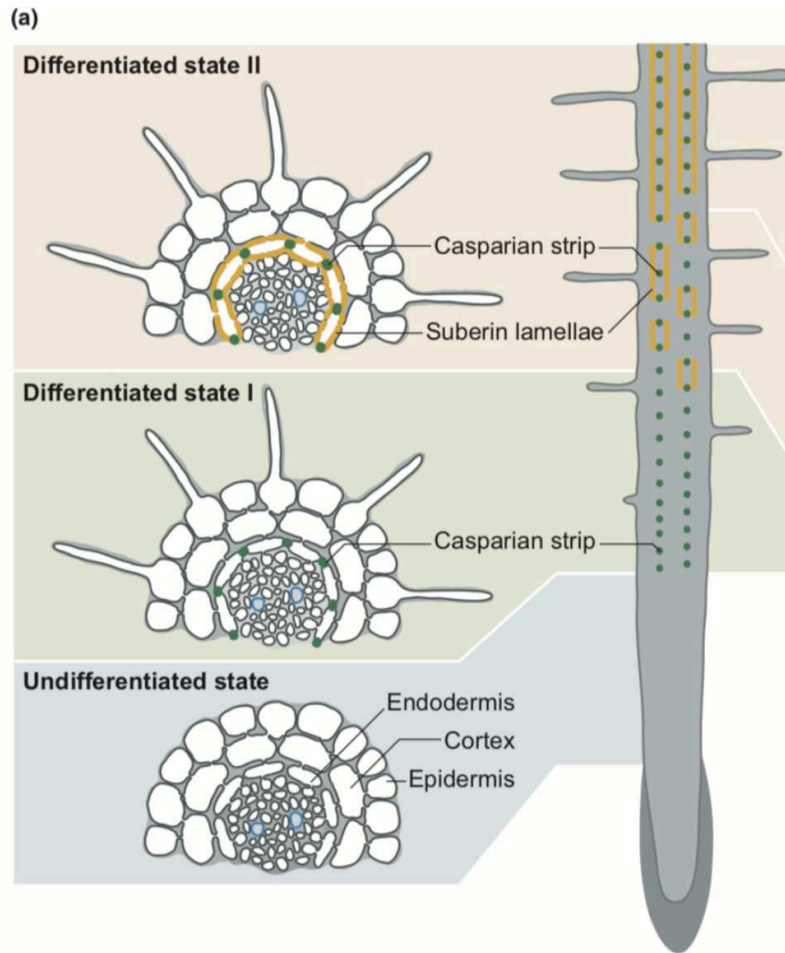
Figure 1.1 Endodermis differentiation. (a) Schematic views of endodermis differentiation, presented as transversal (left panel) and longitudinal views (middle panel) for undifferentiated and states I and II of endodermis differentiation (not at scale). Image reference: Barberon 2017 'The endodermis as a checkpoint for nutrients'.

The optimization of plant barriers in response to a plant's environment is critical to ensure proper nutrient flow for the plant (Ranathunge and Schreiber 2011; Barberon et al. 2016).

Deposition of suberin in the endodermis is responsive to environmental conditions and can be reduced as well as induced. It can be induced by many abiotic stresses such as drought, flooding, salt, and heavy metal such as cadmium (Krishnamurthy et al. 2009; Líška et al. 2016, Shiono et al. 2014). Suberization is increased in response to ABA and decreased in response to

ethylene suggesting the root can return from a protective to absorbent state again (Kosma et al. 2014; Barberon et al. 2016). Overabundance of NaCl and lack of potassium or sulfur in the environment will induce suberization in the endodermis and lack of iron, manganese or zinc will decrease endodermal suberization (Barberon et al. 2016).

The two main polymers in plants responsible for sealing the plant to the outside environment are cutin and suberin. (Schreiber 2010). Both are glycerol-based polyesters with aliphatic monomers. Above-ground plant organs lacking periderm are sealed by the cuticle, a protective film synthesized and secreted by epidermal cells. The cuticle is composed largely of cutin, but may contain some suberin as well, particularly in areas of wounding where suberin will replaced the damaged cutin (Schreiber 2010). Suberin is the sealing component found in roots (endodermis and exodermis), periderm, and the seed coat. Both the cuticle and suberized lamellae or tissues are impregnated with waxes (long chain acyl lipids), however, these waxes are not monomers of either cutin nor suberin and their composition varies. Suberin differs from cutin in its composition of aromatic monomers, mainly alkyl ferulates, coumarates, and caffeates (Schreiber 2010; Domergue and Kosma 2017). The aliphatic monomers of the cutin and suberin differ as well with cutin being composed mostly of C_{16} and C_{18} saturated, oxygenated fatty acids and the aliphatic domain of suberin being composed of saturated and unsaturated oxygenated fatty acids of lengths varying from C_{16} to C_{30} (Matzke and Riederer 1991; Schreiber 2010). The differences found in the aliphatic domain chain lengths and degree of saturation are consistent with the difference in permeability between cutin and suberin. It would be expected that the more permeable of the two, suberin, would contain longer, unsaturated chains which would not pack as tightly as short, saturated hydrocarbon chains (Pollard et al. 2008). Suberin also contains more

glycerol-based aromatic components than cutin (Pollard et al. 2008) which may offset the

hydrophobicity of the longer length aliphatic carbon chains found in the molecule.

Suberin has a very characteristic ultrastructure when deposited as lamellae. As seen with

TEM, micrographs show that suberin is deposited in alternating dark and light bands in cell

lamellae (fig. 1.2c) representing the aliphatic and aromatic domains of the molecule, respectively

(Pollard et al. 2008; Gou et al. 2017). In contrast to cutin, which is deposited on the outside of

epidermal cells, suberin is deposited on the inside of the cell wall in a single or multilayered

lamella between the cell wall and plasma membrane (fig. 1.2) (Robards et al. 1973).
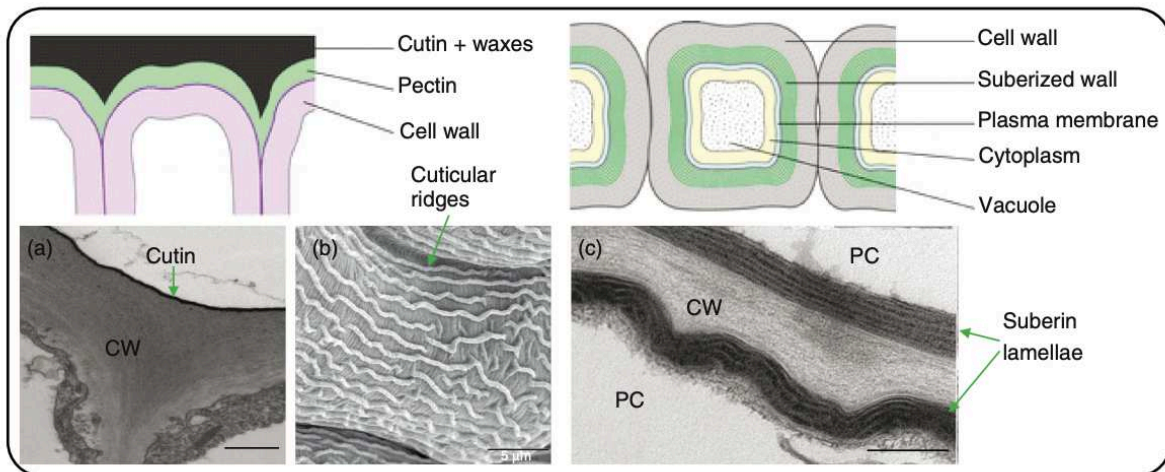
Figure 1.2 'Localization and ultrastructure of cutin and suberin layers. Top panel: Schematic representation of the cuticle (left) and suberized cell wall (right). Bottom panel: Observation of cutin and suberin using electron microscope. (a) Transmission electron microscopy (TEM) image of a cross section view of Arabidopsis stem epidermis. Scale bar: 500 nm. (b) A scanning electron microscopy (SEM) image of the epidermal surface of an Arabidopsis sepal. Scale bar: 5 μm. (c) A TEM image of a cross section view of Arabidopsis roots. Scale bar: 100 nm. Figure from Li-Beisson et al. 2016 'Cutin and Suberin', microscopy by Molina et al. 2009.

Suberin may be deposited within cell walls of root hypodermal, and endodermal cells as well as

the cell walls of cork cells in periderm (Schreiber 2010). In addition to these locations, suberin is

found in the seed coat and produced in areas of wounding or leaf abscission (Molina et al. 2008).

Suberin thus has multiple roles within plants as a barrier. Periderm cork cells and suberized cells which are produced in response to wounding are two suberized cell types that function as impermeable barriers to reduce water loss and prevent pathogen entry. Suberized cells within the endodermis form a dynamic barrier, which may rapidly change based on nutrient availability. Suberin in the endodermis reduces water flow and the Casparian strips and suberin work together to restrict water and nutrient flow from the endodermal apoplast to the endodermal symplast. Because of this, endodermal suberin functions as a barrier to both prevent water loss from the root stele and reduce uptake of harmful ions and molecules into the stele from the cortex (Barberon 2017).

Suberin is also produced in response to wounding where it typically replaces the damaged cuticle (Lashbrooke et al. 2016; Legay et al 2016; Schreiber et al. 2010). Wound suberin is typically less flexible and a poorer water barrier than the cuticle it replaces, however, it must in principle be a better water barrier than the suberin found in root epidermal and endodermal cells which must allow some water to pass through the cell wall (Legay et al. 2016; Pollard et al. 2008; Schreiber et al. 2005). Indeed, the permeability of suberized plant structures can vary due to the composition and quantity of waxes impregnated in the suberin lamella. Wound suberin or suberized periderm cells often have high wax deposition making them less permeable with properties similar to cuticle (Schreiber et al. 2005). In contrast suberized cells in the roots must find a balance between water and nutrient uptake and preventing water loss and may contain much more permeable suberin lamellae due to lower proportion of wax impregnation. In fact, suberin found in the root cell walls of the endodermis and exodermis of several species contains little to no extractable waxes (Schreiber et al. 1999).

Previous work has provided insight to the biosynthesis of suberin. The aliphatic, glycerol, and phenolic monomers must be synthesized independently and then transported to the cell wall where they are enyzmatically polymerized and finally deposited as suberin. Enzymes involved in the biosynthesis of suberin monomers come from many families of enzymes including: ß-ketoacyl-CoA synthases, cytochrome P450 monooxygenases, fatty acyl reductases, glycerol-3-phosphate acyltransferases, and hydroxycinnamoyl-CoA transferases. Suberin is most likely polymerized as soon as it is exported across the plasma membrane, whereas cutin monomers must be transported to the surface of the cell wall before polymerizing. (Phillipe et al 2020; Vishwanath et al 2015).

The fatty acid components of suberin are important for the molecule's hydrophobic properties. C_{16} saturated and C_{18} saturated and unsaturated fatty acids are initially synthesized in the plastid, then transported to the endoplasmic reticulum for elongation and modification. Most of the aliphatic monomers are constructed within the ER. The fatty acids are elongated by ketoacyl-CoA synthases (KCS1 and KCS2) and then modified into primary alcohols by fatty acid reductases (FAR1, FAR4, FAR5), or ω-OH fatty acids by cytochrome p450 monooxygenases (CYP86A1 and CYP86B1). Primary alcohols and ω-OH fatty acids will be used in aromatic oligomer synthesis. Omega-OH fatty acids will also be combined with glycerol in the ER forming 2-monoacylglycerol (2-MAG) 3-phosphate which is the final aliphatic oligomer of suberin (Phillipe et al. 2020; Fernández-Piñán et al 2021).

Aromatic monomer construction takes place in the cytosol where aromatic-CoA molecules are combined with ω-OH fatty acids and primary alcohols produced in the ER forming aliphatic hydroxycinnamates. Alkyl ferulates are produced from feruloyl-CoA via aliphatic suberin feruloyl transferase (ASFT) and alkyl caffeates are produced from caffeoyl-

CoA via fatty alcohol caffeoyl-CoA transferase (FACT). Alkyl coumarates are produced from coumaryl-CoA, but the enzyme responsible is unknown (Phillipe et al. 2020; Fernández-Piñán et al 2021).

Once the aliphatic hydroxycinnamates and 2-MAG 3-phosphate oligomers are formed they are moved to the plasma membrane via the secretory pathway and trafficked through the membrane via ATP-binding cassette G (ABCG) subfamily transport proteins, namely ABCG2, ABCG6, and ABCG20. Once at the cell wall the 2-MAG 3-phosphates must be transesterified and linked to the hydroxycinnamates, however, the process by which the suberin oligomers are polymerized once they arrive at the cell wall is less understood than how the oligomers are synthesized (Phillipe et al. 2020; Fernández-Piñán et al 2021).

The enzymes which polymerize the oligomers most likely belong to the GDSL lipase/esterase (GELP) family, but none have been identified directly as suberin synthases (Yeats et al 2014; Phillepe et al. 2020). Cutin synthase 1 (CUS1), an enzyme from this family, is the only enzyme that has been characterized which is involved in plant polyester polymerization (Yeats et al. 2012). CUS1 has been shown to have high affinity for cutin 2-MAG precursors and to be able to form linear polymers via transesterification of end-chain hydroxyl groups. Tomato mutants lacking CUS1 form a reduced, thin cuticle suggesting the involvement of other enzymes as well (Girard et al. 2012). It is likely that enzymes from the GDSL lipase/esterase family polymerize suberin in a similar manner due to the structural similarities between the two. One piece of support for this is that cutinase, cuticle destruction factor 1 (CDEF1), can degrade both cutin and suberin which highlights the structural similarity of the two and potential similarity between the enzymatic process used to polymerize the respective oligomers of each (Phillepe et al 2020). It should be noted that CDEF1 is part of the same GDSL lipase family which CUS1

belongs to. Although none have been characterized, multiple GDSL lipase/esterase proteins have been shown to be upregulated during suberin synthesis including GELP39, GELP49, GELP51, GELP96 suggesting them as candidates for potential suberin polymerization genes (Phillipe et al. 2020; Fernández-Piñán et al 2021).

1.2 Endodermal differentiation, R2R3-MYB transcription factors and suberin biosynthetic gene expression

In *Arabidopsis thaliana*, the organization of the root is simple, consisting of only a few cell layers formed by a limited number of meristematic divisions. The endodermis in *A. thaliana* is formed when a periclinal division occurs in the cortex-endodermis initial cells, forming the endodermis as the innermost cortical ring of cells (Dolan et al. 1993). The principle function of the endodermis is to regulate ion and water flow in the apoplast and transcellular transport pathways. It is clear that the endodermis functions this way when looking at some of the halophytic plant species, such as salt cress (*Thellungiella halophila*), which contain a multilayered endodermis, one of their adaptations to osmotically stressful soil (Inan et al. 2004). Other plants, such as *Oryza sativa*, contain more complex and diverse cortical cell initials, leading to a more complex pattern of cortical layers in the mature root (Coudert et al. 2010). Many plants contain an additional barrier in the root known as the exodermis. The exodermis is the outermost layer of cortical cells, which contain lignified Casparian strips and suberin lamellae (Peterson and Perumalla 1990). The exodermis provides additional protection from invading pathogens as well as protection from water loss out of the cortex (Enstone et al. 2002). The exodermis functions similar to the endodermis by limiting flow of water and ions through the apoplast and transcellular transport pathways, however, the exodermis restricts flow in and

out of the epidermis and cortex whereas the endodermis restricts flow in and out of the vascular

cylinder and cortex (fig. 1.3) (Enstone et al. 2002).
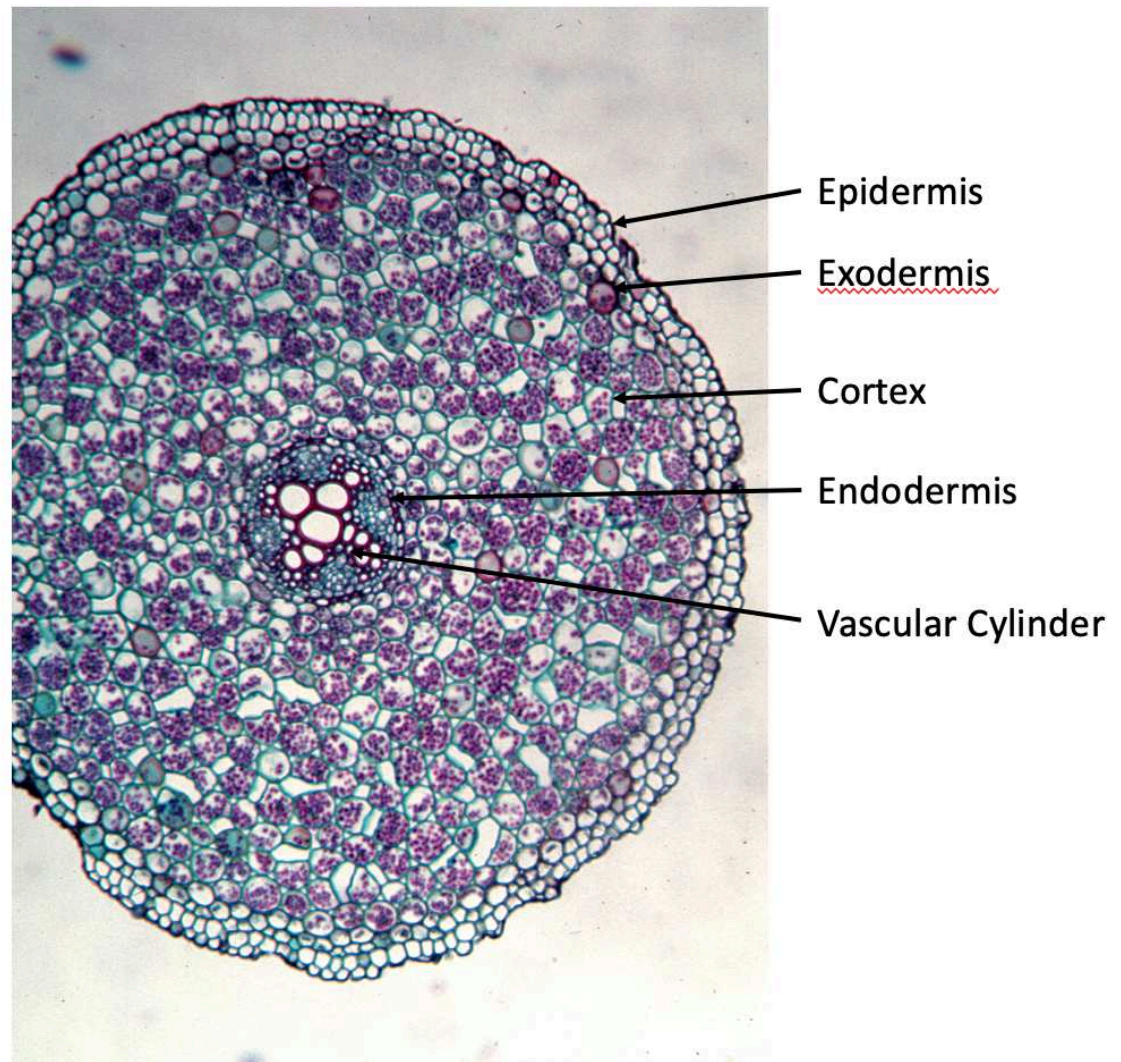
Figure 1.3 Cross section of a *Ranunculus* root showing organization of endodermis and exodermis. Micrograph from Cornell University Plant Anatomy Collection.

During the formation and differentiation of endodermis, the Casparian strips arise first in

development, forming once the barrier cells are fully elongated. Lignin is deposited on the

anticlinal walls which seals the apoplastic space between adjacent endodermal cells. The lignin is

initially deposited in patches which eventually fuse to form a full ring around the endodermis. Formation of the Casparian strips represents state I of endodermal differentiation (Roppollo et al. 2011; Naseer et al. 2012).

State II of root barrier differentiation is the formation of the suberin lamellae. The polymer suberin is deposited along the cell wall in a patch-like manner and will eventually cover all of the primary cell wall resulting in the endodermis providing a barrier to the apoplast and transcellular transport pathways (Robards et al. 1973; Barberon 2017). Although suberin deposition is considered a hallmark of root barrier differentiation state II, suberin is not dependent on the Casparian strip and suberized cells may exist independently such as in tuber periderm. Suberin is not required for the establishment of the apoplasmic barrier and most likely functions to regulate water and nutrients entering the cytoplasm as well as prevent leakage of nutrients and water from the stele (Alassimone et al. 2010; Naseer et al. 2012; Barberon 2016, Barberon 2017).

Differentiation of the endodermis is a genetically regulated process. One of the most critical levels of gene expression regulation is the rate at which genes are transcribed. One way to do this is by altering the strength of the promoter region on the DNA. The protein class known as transcription factors bind DNA at particular sequences in promoter regions, modulating the frequency at which transcription is initiated. Transcription factors are often organized into families based on homology of their DNA binding domains (Latchman 1993). In plants, one of the largest families of transcription factors is the MYB (myeloblastosis) transcription factors. The first MYB transcription factors were identified as part of the avian myeloblastosis virus (Stracke et al. 2001). MYB transcription factors are found in all eukaryotes, however, the family has become greatly divergent in plants (Stracke et al. 2001). MYB transcription factors are

classified based on the number of imperfect MYB repeats in their DNA binding domain. A MYB repeat consists of three alpha helices spanning about 50-55 amino acids, the second and third of which form a helix-turn-helix structure. In plants, MYB transcription factors contain one, two, three, or four repeats. The group of MYB transcription factors containing two repeats, termed the R2R3-MYB transcription factors are unique to plants and with species containing over 100 different R2R3-MYB genes. *Arabidopsis thaliana* contains 126 unique R2R3-MYB transcription factors (Millard et al. 2019).

The function of most of the 126 R2R3-MYB genes is not known, however, of the genes with known function, most of them regulate processes that are unique to plants. R2R3-MYB transcription factors are known to regulate processes such phenylpropanoid biosynthesis, determination of cell identity such as epidermal cell patterning, as well as environmental and hormonal responses (Stracke et al. 2001; Borevitz et al. 2000; Oppenheimer et al. 1991; Lee and Schiefelbein 1999; Byrne et al. 2000). There is no known R2R3-MYB mutant displaying a lethal phenotype and it is unknown whether any of the genes are essential or if redundant functions may be masking the loss of an essential R2R3-MYB gene (Meissner et al. 1999; Stracke et al. 2001).

In the endodermis, the initial differentiation responsible for the establishment of the Casparian strips is regulated by the R2R3-MYB transcription factor AtMYB36. In *A. thaliana*, AtMYB36 is highly expressed in the endodermis during the transition from cell proliferation to cell differentiation. In mutants lacking a functional copy of MYB36, Casparian strip formation is significantly delayed. Additionally, genes associated with endodermal differentiation such as the five *CASP* genes, which are necessary for localizing lignin polymerization proteins to the endodermis, are downregulated. AtMYB36 may also repress genes involved in proliferation of

root ground tissue. In the same mutant lacking functional MYB36, extra cellular divisions were observed in meristematic and differentiation zones of the root. AtMYB36 itself is activated by SCARECROW and SHORTROOT, transcription factors involved in the initial asymmetric divisions in the meristem which forms the endodermis (Liberman et al. 2015).

Several R2R3-MYB transcription factors have been implicated in the transition from the first to the second differentiated state of the endodermis (formation of the suberin lamellae): AtMYB41, AtMYB53, AtMYB92, and AtMYB93 (Shukla et al. 2021). Expression of all of these genes can be induced by ABA, however, AtMYB41 responds the most quickly and strongly to ABA treatment (Shukla et al. 2021). In *Arabidopsis*, most suberin biosynthetic genes are turned on in response to ABA treatment and AtMYB41 is highly expressed in the endodermis in response to ABA treatment (Barberon 2016; Shukla et al. 2021). MYB41 has also been shown to induce suberization in leaves, but not roots when expressed ectopically suggesting that it is post-translationally regulated (Kosma 2014). MYB41 is phosphorylated at serine 251 by MPK6 and that phosphorylation of serine 251 is required for salt tolerance in plant lines overexpressing MYB41 (Hoang et al. 2012). MPK6 expression is induced during salt and drought stress (Hoang et al. 2012 and Tsugama et al. 2012). In a quad mutant lacking functional copies of MYB41, MYB53, MYB92, and MYB93, suberin in the endodermis is almost completely reduced. Furthermore, it remained almost completely reduced in the presence of known activators of suberization such as ABA (Shukla et al. 2021). It is unknown whether or not other R2R3-MYB transcription factors which have been implicated in this process require phosphorylation for activation similar to MYB41.

Additionally, other R2R3-MYB transcription factors may be involved with suberin formation outside of the endodermis. AtMYB67 is highly expressed in the root and predicted *in*

silico to be preferentially expressed in cork tissues making it a potential candidate as a suberin biosynthesis regulators (Czechowski et al. 2004; Rains et al. 2018) and mutants lacking a functional MYB9 contain lower levels of suberin monomers in their seed coats when compared to wildtype *A. thaliana* (Lashbrooke et al. 2016).

In summary, the R2R3-MYB proteins are a large group of transcription factors which are unique to plants. They control many plant specific processes including formation and differentiation of the endodermis. As controllers of these processes, R2R3-MYB transcription factors may be valuable components in synthetic gene circuits which seek to control or refine large scale plant processes.

1.3 Synthetic biology and engineering synthetic plant barriers

Synthetic biology is a field in which biologists seek to redesign existing molecular properties of organisms in order to create new and predictable functionalities for those and other organisms (Khalil and Collins 2010). Sometimes the functions that scientists program into these organisms are entirely novel, such as programming yeast to produce medicines such cannabidiol and artemisinic acid, the precursor to the antimalarial drug artemisinin (Luo et al. 2019; Ro et al. 2006). Other applications may enhance an already existing pathway in an organism.

The field of synthetic biology is hinged on the engineering principles of 'modularization, rationalization, and modeling' (Khalil and Collins 2010). Synthetic circuits are designed *in silico* and then the individual pieces are synthesized and assembled to predictably perform the function the scientist has in mind. The biological circuits are also designed with flexibility in mind. In order to work ubiquitously in different organisms, they are designed to be independent of organism's endogenous regulation pathways (Medford and Prasad 2014).

One aim of synthetic biology is simplicity. A simple circuit is most likely to work predictably and ubiquitously between organisms. Transcription factors can act as a master scale switch for particular cellular processes are thus an attractive target for synthetic biologists. Reconstruction or rewiring of entire transcriptional networks is possible by simply expressing a single transcription factor in a tissue it was not previously expressed in. Synthetic constructs can be created which place transcription factors under control of any known promoter, tailoring the level and location of expression. Furthermore, fully synthetic promoters have been designed, which can give even more control over protein expression (Khalil et al. 2012). These promoters can be made to be inducible using bacterial regulatory elements such as the Tn10-specified tetracycline-resistance operon from *E.* coli (Gossen and Bujard 1992). This system works by inserting a Tet operator between a promoter and a gene of interest. Transcription is suppressed as long as the Tet repressor is bound to the Tet operator, however, upon addition of tetracycline the affinity between the two is disrupted and transcription is allowed to proceed (Gossen and Bujard 1992). These approaches combined (using transcription factors as large scale controllers under control of synthetic and/or inducible promoters) can give scientists almost complete control over where, when, and how often a transcriptional network is turned on or off. As more of these circuits are created, and their components logged in databases, these techniques will become more available to other scientists in turn allowing these methods to become even more precise.

Due to the steady decline in costs for DNA synthesis and sequencing, the applications of synthetic biology are becoming more diverse (Karoui et al. 2019). The advent of new molecular biology tools such as CRISPR and Gibson Assembly have simplified manipulating DNA. CRISPR allows for precise gene editing and Gibson Assembly the simple construction of large plasmids which are assembled from many different molecules of DNA. This is enabling the

synthetic biology field to move towards engineering more complicated organisms such as plants and animals (Wang et al. 2018; Medford and Prasad et al. 2014).

Plants are valuable as both scaffolds for synthetic biology constructs and as sources of components for synthetic biology constructs. Many plant species are easily transformed and plant scientists have united around a few species as models e.g., *Arabidopsis thaliana*. Due to this, large databases of genetic information exist, e.g., The Arabidopsis Information Resource (TAIR). These databases of genetic information can be used as the components of synthetic biology constructs. Quick and easy transformation protocols (e.g., the floral dip technique in *A. thaliana*) make synthetic biology constructs easy to move from bacteria to particular species of plants (*Arabidopsis*, soybean, tobacco, among others), thus making those species amenable as scaffolds for these synthetic constructs.

Synthetic biology gives biologists the tools to direct evolution and implement optimizations where nature has not. For example, it may be possible with synthetic biology to computationally design plant barriers which can allow plants to exist in any environment we choose for them. By taking inspiration from existing adaptations in Kingdom Plantae, such as the multilayered endodermis and exodermis, which allow xerophytic and halophytic species to exist in harsh environments (Inan et al. 2004) and applying synthetic biology principles that allow for predictable behavior to be programmed into plants, there is potential for the above to be accomplished. If synthetic, and highly efficient barriers are engineered into the roots of our staple crop plants such as rice, corn, and soybeans then crop lines can be engineered with potential for greater water-use efficiency, drought-stress tolerance, and pathogen resistance.

For engineering a synthetic barrier in a plant root, the root epidermis is an attractive location. The root epidermis is the main interface with the outside world involved in nutrient and

water acquisition. A synthetic barrier in the root epidermis would function highly similarly to an exodermis, using suberin and lignified Casparian strips to force nutrients and water to pass through membranes which act like filters (Enstone et al. 2002). The exodermis is the outermost layer of the cortex in roots where the cell layer is present (Peterson and Perumalla 1990), however, a root epidermal barrier could turn the outermost layer of cells in the root into a barrier. A synthetic barrier in the root epidermis could then benefit both plants lacking and containing an exodermis by further blocking water and beneficial ion loss from the cortex and blocking pathogen and toxic ion flow into the cortex.

As stated above, several R2R3-MYB transcription factors are implicated in the transition to suberin lamellae formation in the endodermis. In addition to the transcription factors mentioned above (AtMYB41, AtMYB53, AtMYB92, and AtMYB93) other R2R3-MYB transcription factors which are highly expressed in the root and seed coat are likely involved in formation of suberin lamellae. AtMYB67 is highly expressed in the root shown via transcriptomics to be preferentially expressed in cork tissues making it a potential candidate as a suberin biosynthesis regulator (Czechowski et al. 2004; Rains et al. 2018). AtMYB9 may also be involved in suberin lamellae formation as mutants lacking a functional AtMYB9 contain lower levels of suberin monomers in their seed coats when compared to wildtype *A. thaliana* (Lashbrooke et al. 2016).

A critical aspect of engineering plant barriers is understanding the ways in which the plant may modify the barrier in response to environmental conditions. Suberin polymerization is increased in response to ABA and decreased in response to ethylene, both hormones that are used for a variety of environmental responses (Barberon et al. 2016). This means that it is important to consider the environment the plant will be grown in and the purpose the barrier is to

provide. For plants and crops facing the issue of salinity an enhanced suberin barrier in the epidermis is a great solution as these are conditions that typically induce suberization within the endodermis (Kosma et al. 2014; Barberon et al. 2016).

One issue that is often encountered when constructing expression vectors in plants is the issue of endogenous regulation. Many eukaryotic proteins require post-translational modifications such as phosphorylation or methylation in order to change to an active or inactive conformation. Phosphorylation of serine 251 on MYB41 is required for salt tolerance in plants overexpressing the gene (Hoang et al. 2012). It is likely that other R2R3-MYB genes involved in suberin biosynthetic gene activation require phosphorylation as well. One solution to this problem is to make a phosphomimetic protein, a protein that mimics its phosphorylated state via 1-3 amino acid changes (Pitzschke et al. 2014; Medford et al. 2020). By mimicking their phosphorylated state, phosphomimetic proteins can theoretically become constitutively active and maintain their activity in tissues where their native regulatory proteins may not be expressed.

Expression of R2R3-MYB transcription factors must be tissue specific in order to target suberin biosynthesis to a particular area of the root, therefore the promoter controlling a synthetic suberin circuit must belong to a protein expressed solely in the root epidermis. One such class of proteins, ABC transporters involved in root exudation, fit this bill nicely. GFP reporter constructs under control of the AtABCG37 promoter show GFP expression solely in the root epidermis and root hairs of *A. thaliana* plants (Oehmke 2020). *A. thaliana* plants expressing a phosphomimetic MYB41 where serine 251 is mutagenized to aspartic acid under the control of the ABCG37 promoter show a root epidermis and hair covered in suberin when viewed under the microscope with fluorol yellow staining (Medford et al. 2020).

The expression of other R2R3-MYB transcription factors in the root epidermis using the ABCG37 promoter has yet to be tested. R2R3-MYB transcription factors other than MYB41, which have been shown in literature to induce suberization or contain close sequence homology with MYB41 may be able to induce stronger suberization in the root epidermis. In this manuscript, five R2R3-MYB transcription factors, all hypothesized to be involved in transcriptional regulation of suberin biosynthesis, are tested for expression in the root epidermis under control of the ABCG37 promoter. The genes tested include: AtMYB9, AtMYB67, AtMYB92, AtMYB93, and AtMYB102. It should be noted that only an engineered variation of AtMYB102 was tested in this manuscript, rather than the endogenous cDNA as tested of the other genes. This thesis then details the subsequent characterization of the genetic construct containing the MYB92 cDNA under control of the ABCG37 promoter based on its success during initial screening and testing.

Chapter Two: Materials and methods

2.1 Construction of expression vector for root-epidermal specific expression of R2R3-MYB

transcription factors

AtMYB9, AtMYB67, AtMYB92, and AtMYB93 were amplified from pooled

Arabidopsis thaliania Col-0 ecotype cDNA using Phusion polymerase (Thermo Scientific,

Waltham, MA) and primers 1-8 designed in SnapGene (Appendix 2), synthesized by IDT

(Coralville, IA). PCR products were verified for correct length via gel electrophoresis in 1%

agarose gel and then purified using a Qiaquick Gel Extraction Kit (Qiagen, Germantown, MD).

All MYB PCR products were ligated into a pre-existing plasmid backbone containing the pABC

transporter 5' of the MYB gene inserts and the NOS terminator 3' to the MYB gene inserts (fig.

2.1). The existing cassette of AtmCherry and its linked gene were digested out using BamHI and

Eco53KI (NEB, Ipswitch, MA).
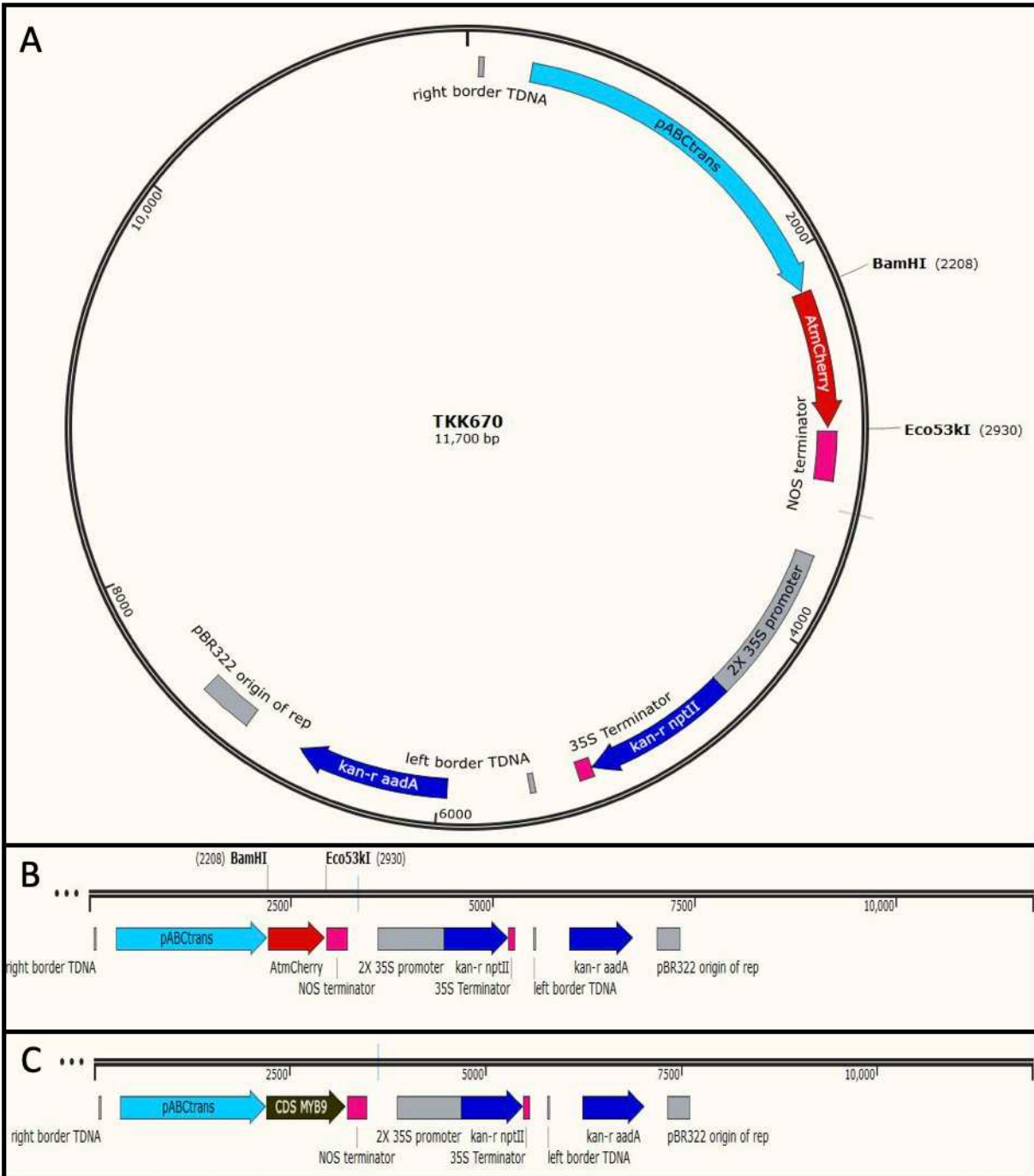
Figure 2.1 Vector maps of TKK670 and NTB009 constructs. **A**. Circular map of TKK670 plasmid. Restriction sites shown used to linearize plasmid for backbone in suberin/MYB TF circuits. **B**. Linear map of TKK670 construct. **C**. Linear map of NTB009 construct. All NTB constructs are identical except that they contain the coding sequences of their respective MYB transcription factors instead of the MYB9 coding sequence.

NTB092 was constructed using Gibson Assembly with the digested plasmid backbone of TKK670 (fig. 2.1) and PCR product of MYB92 using a NEB Gibson Assembly Cloning Kit (NEB, Ipswitch, MA). MYB92 PCR product was generated using cloning primers 5 and 6 (Appendix 2) and the Gibson Assembly reaction was carried out using primers 12 and 13 generated by the NEBuilder primer design tool (NEB, Ipswitch, MA; Appendix 2). NTB067 and NTB009 were constructed using a two-step PCR process followed by BamHI digestion and ligation using T4 DNA ligase (NEB, Ipswitch, MA) according to the NEB T4 DNA ligase protocol (NEB). MYB67 and MYB9 were first amplified using PCR with cloning primers. A second round of PCR amplification was carried out using the first product as template and a new 5' primer containing a BamH1 site (primers 10 and 11). These products were digested with BamHI and ligated into the digested TKK670 backbone. Ligations were carried out using a 5:1 stoichiometric ratio of insert to backbone and required masses were calculated using NEBioCalculator (NEB). NTB093 was constructed by amplifying MYB93 in a Phusion PCR reaction using cloning primers 7 and 8 (Appendix 2) and ligating into a pMini2.0 cloning vector (Appendix 3) from a NEB PCR Cloning Kit (NEB, Ipswitch, MA). BamHI and ZraI (NEB, Ipswitch, MA) were used to digest MYB93 from the multi-cloning site of pMini2.0 and the two fragments were separated using gel electrophoresis with 1% agarose gel. The band containing MYB93 at about 1000 bp was purified with the Qiagen Gel Extraction Kit and this fragment was ligated into the digested TKK670 backbone following the same procedure as above.

2.2 Site-directed mutagenesis and construction of phosphomimic expression vectors

The site-directed mutagenesis reactions in order to change threonine 274 and serine 278 of AtMYB67 and threonine 301 and serine 305 of AtMYB102 into aspartic acid residues was carried out using a NEB Q5 Site-directed Mutagenesis kit (NEB, Ipswitch, MA) according to the

protocol in the kit. The primers (14-21) were designed using the NEBaseChanger tool online and the sequences can be found in the appendix (Appendix 2). Two different vectors were used as templates for the reaction: pMini2.0 MYB67 and pENTR MYB102 (Appendix 3).

Transformation was done according to the above kit protocol and then 2-3 colonies per reaction were chosen and grown in liquid LB media with kanamycin (50ng/mL) or carbenicillin (50ng/mL), depending on the respective vector resistance, overnight at 37° C. Plasmids were isolated from liquid cultures using a Qiagen QiaPrep Spin Miniprep Kit (Qiagen, Germantown, MD). Isolated plasmids were prepped for Sanger sequencing by combining 631 ng plasmid with 15 pmol of reverse cloning primer (Appendix 2) in a 15 µL reaction. Sanger sequencing was carried out by GeneWiz (South Plainfield, NJ). Sanger sequencing results were aligned to the reaction template using SnapGene and the trace chromatogram was analyzed to confirm the proper mutagenesis reaction occurred.

Once the desired amino acid change was evaluated in SnapGene, the mutagenized MYB genes were cloned into the plant expression vector (table 2.2). Mutagenized MYB67 was cloned into TKK670 backbone in the same manner as was described in section 2.2.1, except that the template for the first round of PCR was the plasmid containing the successful mutagenesis reaction instead of pooled *A. thaliana* cDNA. Mutagenized MYB102 was cloned into the TKK670 backbone in the same manner. Due to MYB102 containing an internal BamHI site, a 5' primer containing a BglII site was used instead of a primer containing a 5' BamHI site. BglII sticky ends are compatible with BamHI, allowing the mutagenized MYB102 PCR product to be ligated into the TKK670 backbone.

2.3 Transformation of plant expression vectors into *E. Coli* and *Agrobacterium* competent cells and screening of *E. Coli* transformants

Recombinant plasmids were transformed into DH5-α or 10-β competent *E. coli* cells and GV3101 competent *Agrobacterium tumefaciens* cells. Chemically competent 10- β cells were purchased from New England Biolabs (Ipswitch, MA). Electrocompetent DH5-α *E. coli* and GV3101 *Agrobacterium* cells were generated according to the protocol by Gonzalez et al. 2013. Ten-beta cells were used according to the protocol in the NEB PCR cloning kit (NEB, Ipswitch, MA). Electrocompetent cells were electroporated using a ECM630 Electro Cell Manipulator (Harvard Apparatus, Holliston, MA) in electroporation cuvettes (89047-206, VWR, Radnor, PA) containing 1-3µL ligation mixture and 50µL competent cells. *E. coli* competent cells were electroporated at 1250 v, 200 Ω, and 25 µF. *Agrobacterium* competent cells were electroporated at 1800 v, 200 Ω, and 25 µF. Following electroporation *E. coli* cells were placed immediately in 1mL of SOC or LB media and allowed to recover for 1hr at 37˚C. Following recovery, *E. coli* was plated for selection on LB media containing 50 ng/mL kanamycin. *Agrobacterium* cells were placed in 1 mL LB media and allowed to recover for 1hr at 28˚C, then plated for selection on LB media containing 15 ng/mL rifampicin, 50 ng/mL gentamicin, and 50 ng/mL kanamycin.

Resulting *E. coli* colonies from plasmid transformation were screened via PCR amplification using GoTaq polymerase and forward and reverse primers used to initially generate MYB gene fragments. Plasmids from positive colonies were isolated using a Qiaprep MiniPrep Spin kit or Qiacube MiniPrep procedure (Qiagen, Germantown, MD). MYB genes of resulting plasmids were sequenced using Sanger sequencing by GeneWiz using a promoter specific primer (primer 9, Appendix 2) (in order to sequence the promoter/coding sequence junction) and their respective reverse cloning primers.

2.4 Transformation of *Arabidopsis* via floral dip and plant growth conditions

Col-0 plants were prepared and transformed using the floral dip method following the protocol by Rivero et al. 2014. Five mL GV30101 *Agrobacterium* competent cell cultures were grown overnight on a shaking incubator at 28°C in liquid LB media containing 15 ng/mL rifampicin, 50 ng/mL gentamicin, and 50 ng/mL kanamycin. One mL of culture was pipetted into 500 mL of fresh liquid LB media with the same antibiotic concentrations and grown overnight on a shaking incubator at 28°C. Cultures were centrifuged in a Beckman (Indianapolis, IN) J2-21M centrifuge for 15 minutes at greater than 4000x g at room temperature and resuspended in 1000 mL new infiltration media (50 g sucrose/L H_2O and 0.203 g $MgCl_2$/L H_2O) in a 5 L bucket. Silwet L-77 (PlantMedia, Irving, TX) was added to concentration of 0.02%. 12-16 plants (3-4 pots) were dipped for each genetic construct for 3-5 minutes then placed sideways on wet paper towels and covered with plastic wrap overnight. Plants were dipped again 7 days later, following the same protocol in order to increase transformation efficiency.

In preparation for floral dip protocol Col-0 ecotype *A. thaliana* was plated on MS agar media and grown under short day conditions (eight hours light, 16 hours dark, about 13,000 lux). Once between the size of a nickel and quarter plants were moved to soil in four inch pots, four plants to a pot. Col-0 was grown for 3-4 weeks before being moved to long day conditions. Terminal inflorescences were clipped and lateral inflorescences were allowed to grow for about a week before dipping. Following harvest and sterilization of seed using 70% EtOH for two minutes and 50% bleach for 10 minutes T_0 plants were selected for by growth on MS agar media containing 50 ng/mL kanamycin and 100 ng/mL cefotaxime. T_0 plants were grown on vertical plates for screening, following selection, and then transferred to soil in two inch pots and grown under long day conditions on racks in a growth room. T_1 and T_2 seeds were germinated on MS

media containing 50 ng/mL kanamycin under long day conditions and then transferred to two inch pots under long day conditions unless otherwise specified.

2.5 T_0 transgenic plant screening

Seedlings were grown on vertical MS agar plates containing 50 ng/mL kanamycin and 100 ng/mL cefotaxime for between 8-10 days. One vertical plate containing Col-0 was grown on MS agar with no antibiotics as a control. Plants were removed from plates and a single root was excised using scissors and placed into a multi-well (6, 12, or 24) plate. The plant was then rescued onto a large round MS agar plate containing the same antibiotic composition as above to be grown for seed. 0.01% Fluorol Yellow 088 solution was created by dissolving 5 mg Fluorol Yellow 088 powder in 50 mL lactic acid. Roots were stained for 30 min in Fluorol Yellow solution at 70° C. Roots were then rinsed in DI water three times for 10 minutes each while shaking at about 100 rpm on a shaking table. Samples were kept in the dark and discarded after three hours to avoid bleaching and/or signal leaking (Lux et al. 2005).

Samples were viewed under a Leica DM5000B microscope (Leica, Wetzlar, Germany) using a GFP filter. Fluorol Yellow 088 is excited at 450 nm and has emission at 515 nm. The areas of the root viewed during screening were: root apical meristem, the elongation zone, the maturation zone, lateral roots, root hairs, and the root to shoot transition zone. Transgenic roots were screened based on perception of signal in the epidermis relative to wildtype Col-0 *Arabidopsis* roots of the same age grown on vertical plates. Several individual transgenic lines that had been selected for using kanamycin were screened for each construct. Image acquisition for screening was done using a Leica DFC450 microscope camera (Leica, Wetzlar, Germany).

2.6 Establishment of stable-homozygous transgenic plant lines

Following screening, between 3-5 independent transgenic lines from each construct screened were selected for further study and put to soil to collect seed. Plants were grown individually in two-inch pots under long day conditions. Plants were harvested and inflorescences, fruits, and seeds were dried in bags for 2-3 days before collection using a sieve. The collected T1 seeds were plated on MS agar plates containing 50 ng/mL kanamycin with a density of 50 seeds/plate. Seeds were in darkness at 4° C for three days to vernalize then grown under long-day conditions (16 hours light, eight hours dark, about 13,000 lux). Transgene segregation was observed by counting alive (kanamycin resistant) seedlings after two weeks. Chi-square tests were used to determine if the ratio of kanamycin sensitive plants and kanamycin resistant plants are in agreement with Mendelian genetics. A plant is homozygous once all progeny are kanamycin resistant. If all T_1 lines for a particular construct were heterozygous then about six kanamycin resistant plants were chosen to be grown to seed in order to determine transgene segregation of their progeny. The T_2 seeds were then plated at the same density (50 seeds per plate) to determine the ratio of kanamycin resistance and kanamycin sensitivity.

2.7 Characterization of homozygous plant lines (NTB092)

2.7.1 Microscopy

Col-0 was grown 10 days under long day conditions on MS agar media. Transgenic plants were grown for 10 days under long day conditions on MS agar media containing 50 ng/mL kanamycin. Roots were clipped just above the root to shoot transition zone and stained using Fluorol Yellow 088 stain in the same manner as the protocol described in section 2.5. Following staining, whole roots were mounted in 50% glycerol.

Samples were viewed using a Leica DM5000B microscope (Leica, Wetzlar, Germany) with GFP filter. Flurol Yellow 088 is excited at 450 nm and has emission at 515 nm. The following root zones were analyzed in each sample: root to shoot transition zone, maturation zone, elongation zone, root tip. Col-0 was used as a negative control as it lacks epidermal suberin in the root except for a small amount in the root to shoot transition zone, the periderm region. Image acquisition for characterization of homozygous transgenic lines was done using a Leica K5 sCMOS microscope camera (Leica, Wetzlar, Germany).

2.7.2 ABA and ACC plant treatments

Col-0 was grown either 10 or 11 days on MS agar media under long day conditions. Transgenic plants were grown 10 or 11 days on MS agar media containing 50 ng/mL kanamycin. Plants grown 10 days were re-plated on MS agar media containing 2 μM 1-aminocyclopropane-1-carboxylic acid (ACC) and treated for 48 hours. Plants grown 11 days were re-plated on MS agar containing 1 μM abscisic acid (ABA) and treated for 24 hours. Following treatment, plants were analyzed using microscopy according to the same protocol described in section 2.5.

2.7.3 Measurement of root length

Col-0 plants and transgenic plants were grown for 14 days on vertical plates with MS agar and 50 ng/mL kanamycin MS agar respectively. Root tips were marked with a marker and measured in millimeters using a ruler. Significance of datasets was evaulated using student's T-test.

2.7.4 RT-qPCR of Col-0 and NTB092

Three cDNA libraries were constructed for both Col-0 and NTB092. Roots of 21 plants were used in the construction of each library. Pooled roots were frozen in liquid nitrogen and

pulverized using a tissue homogenizer. Total RNA was extracted using Trizol phenol-chloroform extraction method (Rio et al. 2010). The method relies on the Trizol reagent which solubilizes biological material and the addition of chloroform to separate protein, DNA, and RNA into different phases. First-strand cDNA synthesis was done using a Verso cDNA synthesis kit (Thermo Fisher Scientific, Waltham, MA), using oligo dT primers for mRNA selection.

Each cDNA library was used as a biological replicate for qPCR. Four technical replicates were done of each biological replicate. The housekeeping gene actin (ACT2) was used as a calibration control for the target genes as it is expressed constitutively in all tissues. Target genes included: FACT, ABCG6, KCS2, GELP51. All PCR products were 120 bp long. Samples were loaded using Lightcycler I SYBR Green Master Mix (Roche, Indianapolis, IN). and run on a BioRad CFX96 thermocycler (Biorad, Hercules, CA). Ct values were analyzed using the delta-delta Ct method using Col-0 delta Ct values as the calibration group. Error was determined by calculating the standard deviation of the fold change for control and transgenic groups. Significance of results was determined using student's T-test.

Table 2.1 Vectors used during cloning

Purpose	Construct name	Construct description (5'→3')	Restriction enzymes used	Cloned fragment	Removed fragment
Source of pABCG37, NOS terminator, 2x 35S promoter, kan-r nptiii, 35s terminator, kan-r aadA, and pBR322 origin of replication.	TKK670	pABCG37::mCherry::TNOS, 2xp35S::kanr nptII::T35S, kanr aadA, pBR322 origin of replication	Bam HI, Eco53KI	pABCG37::TNOS, 2xp35S::kanr nptII::T35S, kanr aadA, pBR322 origin of replication	mCherry
Sub clone of NTB093	pMini2.0 MYB93	SP6 promoter::MYB93, T7 promoter::AmpR	BamHI, ZraI	MYB93	SP6, T7::AmpR
Final clone	NTB009	pABCG37::MYB93::TNOS, 2xp35S::kanr nptII::T35S, kanr aadA, pBR322 origin of replication	-	-	-
Final clone	NTB067	pABCG37::MYB67::TNOS, 2xp35S::kanr nptII::T35S, kanr aadA, pBR322 origin of replication	-	-	-
Final clone	NTB092	pABCG37::MYB92::TNOS, 2xp35S::kanr nptII::T35S, kanr aadA, pBR322 origin of replication	-	-	-
Final clone	NTB093	pABCG37::MYB93::TNOS, 2xp35S::kanr nptII::T35S, kanr aadA, pBR322 origin of replication	-	-	-

Table 2.2 Vectors used during construction of phosphomimic constructs

Purpose	Construct name	Construct description (5'→3')	Restriction site added to 5' side of PCR fragment
Provided a smaller plasmid for mutagenizing MYB67. PCR template for cloning to expression vector.	pMini2.0 MYB67	SP6 promoter::MYB67, T7 promoter::AmpR	BamHI
Provided a smaller plasmid for mutagenizing MYB102. PCR template for cloning to expression vector.	pENTR MYB102	T7 promoter::KanR, rrnB T2 terminator, rrnB T1 terminator, MYB102	BglII
Final clone	NTB067S	pABCG37::MYB67^{278D}::TNOS, 2xp35S::kanr nptII::T35S, kanr aadA, pBR322 origin of replication	-
Final clone	NTB067T	pABCG37::MYB67^{274D}::TNOS, 2xp35S::kanr nptII::T35S, kanr aadA, pBR322 origin of replication	-
Final clone	NTB102S	pABCG37::MYB102^{305D}::TNOS, 2xp35S::kanr nptII::T35S, kanr aadA, pBR322 origin of replication	-
Final clone	NTB102T	pABCG37::MYB102^{301D}::TNOS, 2xp35S::kanr nptII::T35S, kanr aadA, pBR322 origin of replication	-

Chapter Three: Results

3.1 Screening of T_0 plants for epidermal suberin

T_0 plants (independent transformants) were screened for epidermal suberin using fluorescence microscopy with Fluorol Yellow 088 (FY) stain and Col-0 ecotype *A. thaliana* as a control. In Col-0 roots, suberin is found only in the endodermis; therefore FY signal is found only there. To screen transformants, their epidermal FY signal was rated on a -,+, or ++ scale. All screening data is summarized in table 3.1.

Table 3.1 Preliminary Suberin screening results and notes from T_0 (primary) transgenic generation plants

Construct name and corresponding MYB gene	Number of independent transgenic lines screened	Number of transgenic lines with +,++ fluorol yellow signal in epidermis	Notes
NTB009 (MYB9)	19	1	Epidermis identical to Col-0 in almost all cases. Some plants with signal in root tips.
NTB067 (MYB67)	16	5	High signal in young root epidermis and low or patchy signal in mature root. Lateral root epidermis observed with high signal.
NTB092 (MYB92)	16	7	Signal variable throughout root. Consistent signal found in lateral roots and junctions. Mix of high and low signal in epidermis in primary root.

Construct name and corresponding MYB gene	Number of independent transgenic lines screened	Number of transgenic lines with +,++ fluorol yellow signal in epidermis	Notes
NTB093 (MYB93)	19	16	Many plants with signal in root epidermis. Fluorol Yellow signal seen in epidermal cell junctions throughout much of root.
NTB067S (MYB67 serine 278 to aspartic acid)	21	3	Nearly identical to NTB067.
NTB067T (MYB67 threonine 274 to aspartic acid)	7	0	Nearly identical to NTB067
NTB102S (MYB102 serine 305 to aspartic acid)	0	0	MYB102 gene expression is consistent with a lethal phenotype.
NTB102T (MYB102 threonine 301 to aspartic acid)	0	0	MYB102 gene expression is consistent with a lethal phenotype.

Of the six epidermally targeted MYB genes, I examined at least seven independent transgenic lines per MYB gene construct. The exact numbers of independent lines per MYB construct examined are found in table 3.1. The MYB92 construct exhibited the highest number of + and ++ independent transgenic lines, independent line numbers 12 and 21 being the most notable. Initially, I thought that the NTB093 plants had the greatest number of + and ++ rated transgenic lines, however, upon reevaluation of the two independent homozygous lines selected, they were found to be false positives. The two lines were selected because I had initially thought

they had the most abundant epidermal FY signal of the 19 independent lines initially screened.

One of the false positive lines contained a single T-DNA insertion of MYB93 (NTB093.07) and

the other contained two T-DNA insertions of MYB93 (NTB093.08), as verified by chi-square

analysis (table 3.2) Due to T-DNA insertions commonly being epigenetically silenced, I

reanalyzed the T_1 heterozygous NTB093.07 line. There was little to no epidermal suberin in this

line, therefore it was concluded that these lines were false positives for epidermal suberin, and

that gene dosage in the homozygous lines of NTB093 was not causing epigenetic silencing.

Screening of the MYB transgenic lines took place using a different camera than the

characterization of the homozygous MYB lines (section 2.5 and 2.7.1). The camera used for

characterization made identification of false positive lines much easier.

Because Fluorol Yellow 088 stains lipids, and not specifically suberin, false positive

screens may have occurred in all lines screened. Additional variation in the assay could result

from other variables in the staining process as well. There may be slight differences in stain

concentration due to variation in measurement while making the stain, as well as volume of

water used to wash the stain. Some samples are washed longer than others as the stain/water is

emptied from the plate wells one by one. This may have been the case in the lines containing the

NTB009 and NTB067 construct as well in which 1/19 and 5/16 independent transgenic lines

respectively were given + or ++ ratings. Another possibility is that the respective MYB genes in

these constructs only weakly establish suberin production in a limited number of cells. After the

more rigorous evaluation of the independent transgenic lines initially selected during preliminary

screening, only plants expressing MYB92 were chosen for further characterization.

Four engineered constructs were also independently transformed into plants: NTB067S,

NTB067T, NTB102S, and NTB102T. The constructs were engineered for amino acid changes at

threonine 274 (NTB067T) and serine 278 (NTB067S) in MYB67 and threonine 301(NTB102T)

and serine 305 (NTB102S) in MYB102. In all cases these amino acids were mutagenized to

aspartic acid which could mimic the effect of phosphorylation. Transformants with the two

putative phosphomimics, NTB067S and NTB067T, looked identical to those of NTB067.

NTB067S had 3/21 + or ++ ratings and NTB067T had 0/7 + or ++ ratings. The portion of

positive/negative screens may be smaller in these constructs than NTB067 due to an increased

ability to detect false positives during screening. Upon transformation of NTB102S and

NTB102T into Col-0 plants, zero transformants were recovered, consistent with the constructs

being lethal to seedlings or *Agrobacterium tumefaciens*. T_0 generation NTB102S and NTB102

lines were plated at least 10 times, with hundreds of potential independent transformants on each

plate. Not one kanamycin resistant line was recovered. Because none of the phosphomimic lines

were found to have clear positive signal in the epidermis, no lines were selected to be further

characterized.

Table 3.2 Chi-square analysis of genetic segregation of single T-DNA insertions in T_1 generation transgenic lines

Transgenic line	Total progeny observed	Number of progeny kanmycin resistant	Number of progeny kanamycin sensitive	χ^2 value	Hypothesis accepted (1 T-DNA insertion)
NTB092.12	50	35	15	0.67	Yes
NTB092.21	50	39	11	0.24	Yes
NTB093.07	50	40	10	0.67	Yes
NTB093.08	50	48	2	11.76	No, χ^2=0.43 for two T-DNA insertion hypothesis

The lines selected for characterization following screening were chosen based on high rating of FY signal during microscopy as well as a chlorotic, stunted phenotype (fig 3.01). I hypothesized that this phenotype is occurring due to the ectopic suberin limiting flow of nutrients across the root epidermis. The NTB092 construct, expressing MYB92 in the root epidermis shows strong FY signal in the root epidermis and plants containing this construct are stunted in both root and shoot size, and shoots exhibit chlorosis. Plants containing the NTB092 construct were the only plants to exhibit both strong signal in the root epidermis as well as the chlorosis phenotype.
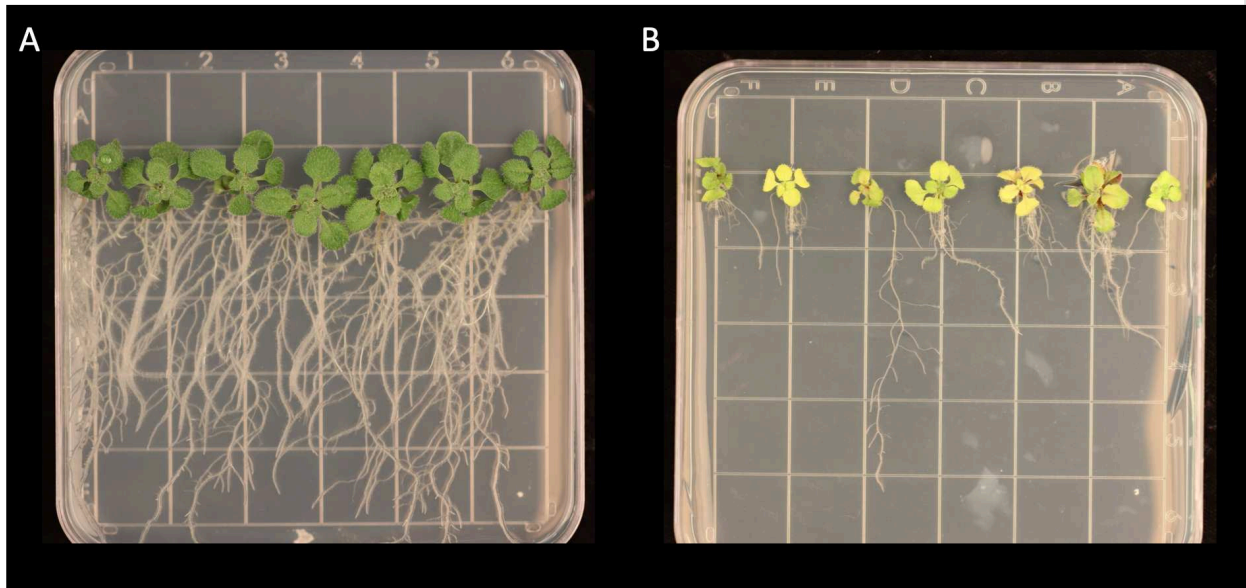
Figure 3.01 Chlorosis and stunted phenotype of plants expressing MYB92 in root epidermis. **A.** Fourteen-day old Col-0 ecotype *A. thaliana*. **B.** Fourteen-day old *A. thaliana* containing the NTB092 construct.

Figure 3.02 Stunted phenotype of plants expressing MYB92 in root epidermis. Once put to soil transgenic plants mostly recover from chlorosis. **A.** Col-0; **B.** NTB092.

3.2 Fluorescence microscopy of transgenic lines homozygous for MYB92 T-DNA insertion

Because transgenic plants containing the NTB092 construct met the criteria defined in section 3.1, clear epidermal FY signal and a chlorotic, stunted phenotype, homozygous progeny were selected and ten to fourteen day old plants were used for further study. The two independent lines of NTB092 are single T-DNA insertions as verified by chi-square analysis (table 3.2). Seeds of each transgenic line were plated 50 at a time for genetic analysis. In a homozygous line all 50 seeds are resistant to kanamycin. Homozygous lines have less than a one in ten thousand chance to exhibit a 3:1 kanamycin resistance to sensitivity ratio. Ten to fourteen days old NTB092 and Col-0 *Arabidopsis thaliana* were used for characterization via

fluorescence microscopy. Both tap roots and lateral roots were analyzed in the zones listed in

figure 3.03. Consistently, NTB092 plants exhibit lateral roots with suberized epidermis. The

taproots in NTB092 plants appear similar to those of Col-0 in some cases exhibiting suberin in

the endodermis and lacking it in the epidermis. In some cases, the taproot epidermis is also

suberized suggesting environmental and microenvironmental feedback is affecting the

expression of MYB92 in the root epidermis.
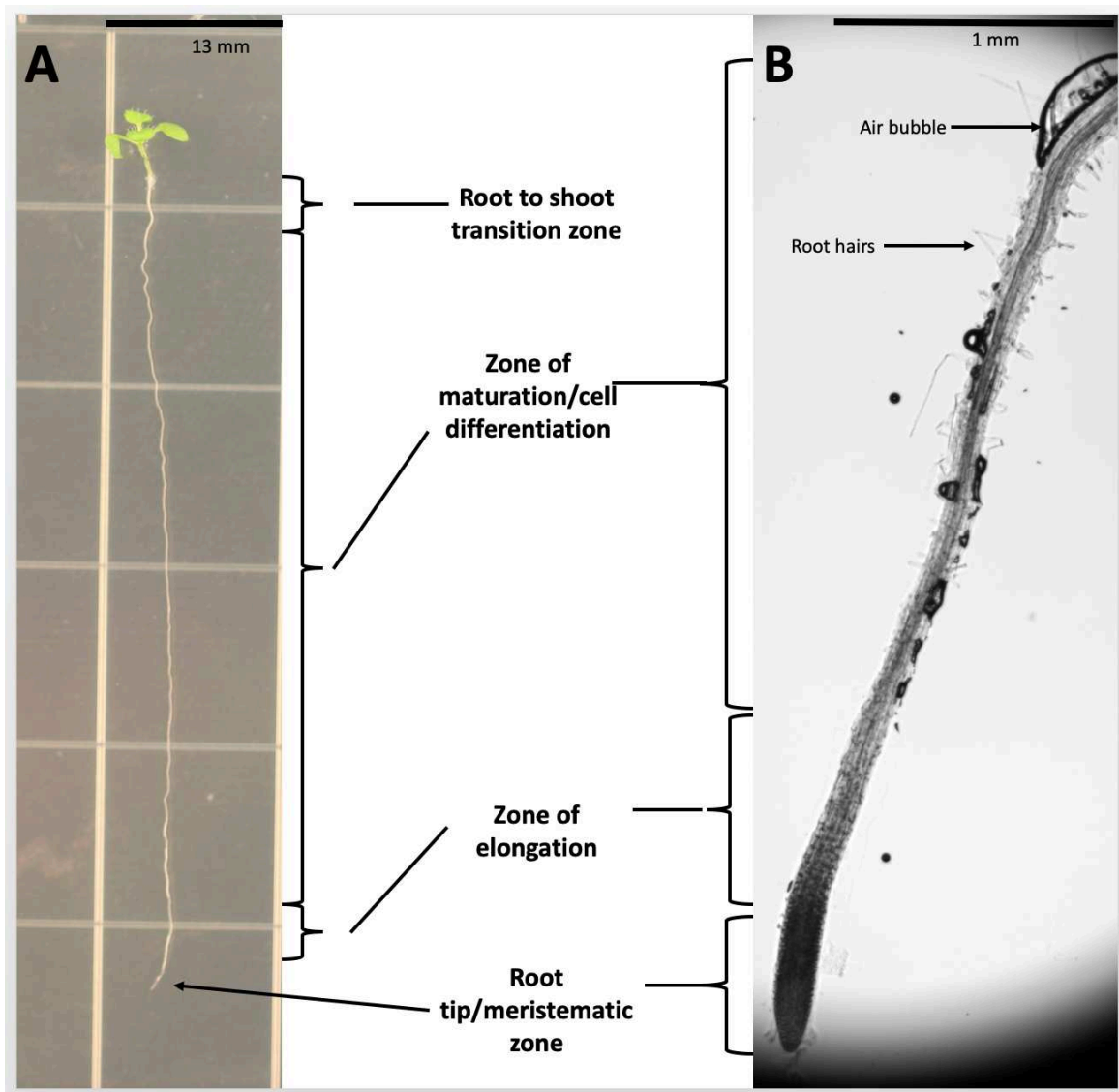
Figure 3.03 Diagram of root zones observed during fluorescence microscopy. **A.** Photograph of *Arabidopsis* root. **B.** Micrograph of *Arabidopsis* root tip.

In the root to shoot transition zone, both NTB092 and Col-0 show a strong central FY signal due to suberin in the endodermis (fig. 3.04). Additionally, strong FY signal can be observed in cell junctions across the root to shoot transition zone due to suberin forming in what will eventually be a small amount of periderm in the root to shoot transition zone. Equal exposure micrographs of NTB092 and Col-0 root to shoot transition zones suggest that the suberin levels are approximately equal in this zone.

In the root maturation zone, epidermal cells and root hairs of NTB092 are suberized as seen by FY signal whereas Col-0 plants lack signal in the epidermis (fig. 3.05). Relative strength of FY signal between NTB092 plants is variable suggesting variation caused by the FY staining process. FY signal is higher in the endodermis relative to the epidermis suggesting endogenously suberized cells are suberized to a greater degree than transgenically suberized cells (fig. 3.05E,F,G).

In the root elongation zone, FY signal from NTB092 plants and Col-0 plants is similar (fig. 3.06). Strong FY signal is not observed in the epidermis of either transgenic or wild type plants, while weak, hard to quantify signal was seen in the NTB092 epidermis (fig. 3.06E). One possibility is that, due to the rapid expansion of cells in the elongation zone, the relative amount of suberin is depleted here. FY is seen throughout the endodermis, with FY signal diminishing near the distal end of the root, typical of endodermal cells in this zone (fig. 3.06).

One region where NTB092 consistently showed strong epidermal suberin was in lateral roots. Lateral roots of NTB092 plants consistently show suberized epidermal cells (fig. 3.07e and 3.08e). In both Col-0 and NTB092 roots, suberin can be observed at the base of lateral roots just as they emerge through the epidermis (fig. 3.07). FY signal can be observed in NTB092

throughout lateral roots, whereas it is only seen at the base of the emerging lateral root in Col-0 (fig. 3.07).

In mature lateral roots of NTB092 suberin in the epidermal cells is consistently found to be deposited in a diffuse manner (fig. 3.08 and 3.09). The signal at the base of the lateral root (as above) persists in both Col-0 and NTB092 mature lateral roots. In both types of lateral roots the endodermis is clearly defined by FY signal. However, in NTB092 roots there is clear FY signal around epidermal cell junctions throughout the length of the maturation zone (fig. 3.08E,F,H; fig.3.09A,B). In Col-0 roots there is a clear absence of signal in this location in this zone (fig. 3.08A,B,C,G).

Multiple homozygous lines of NTB092 (NTB092.12 and NTB092.21) were created and evaluated in order to determine that MYB92 expression in the root epidermis is responsible for the observed phenotypes of epidermal suberin, chlorosis, and stunted roots and shoots. The independent transgenic lines contain distinct insertions of the NTB092 construct, verified by chi-square analysis to be single copy, and verified for homozygous progeny (all progeny kanamycin resistant). Use of multiple independent transgenic plants assures that the phenotypes are not due to mutagenesis at the specific T-DNA insertion site. Comparitively, the two transgenic lines are similar in regards to phenotype (fig. 3.10). Both contain epidermal suberin as seen via FY signal in epidermal cells as well as the stunted and chlorosis phenotype (fig. 3.01 and 3.10). Intensity of FY signal is comparable between NTB092.12 and NTB092.21 lines, however, NTB092.21 appears to contain more epidermal suberin in particular locations such as root hairs (fig. 3.10). NTB092.12 plants exhibit chlorosis of shoots, however, the chlorosis is limited to the edge of leaves or is patchy in appearance. In NTB092.21 plants the whole shoot in many cases is chlorotic (fig. 3.01B). Plants are stunted in size in both lines, but NTB092.21 plants are more

stunted than their NTB092.12 counterparts. Interestingly, once put to soil from plates,

NTB092.21 plants recover from their chlorosis (fig 3.02B). This might be due to the reduced

osmotic potential of soil when compared to full strength MS media.
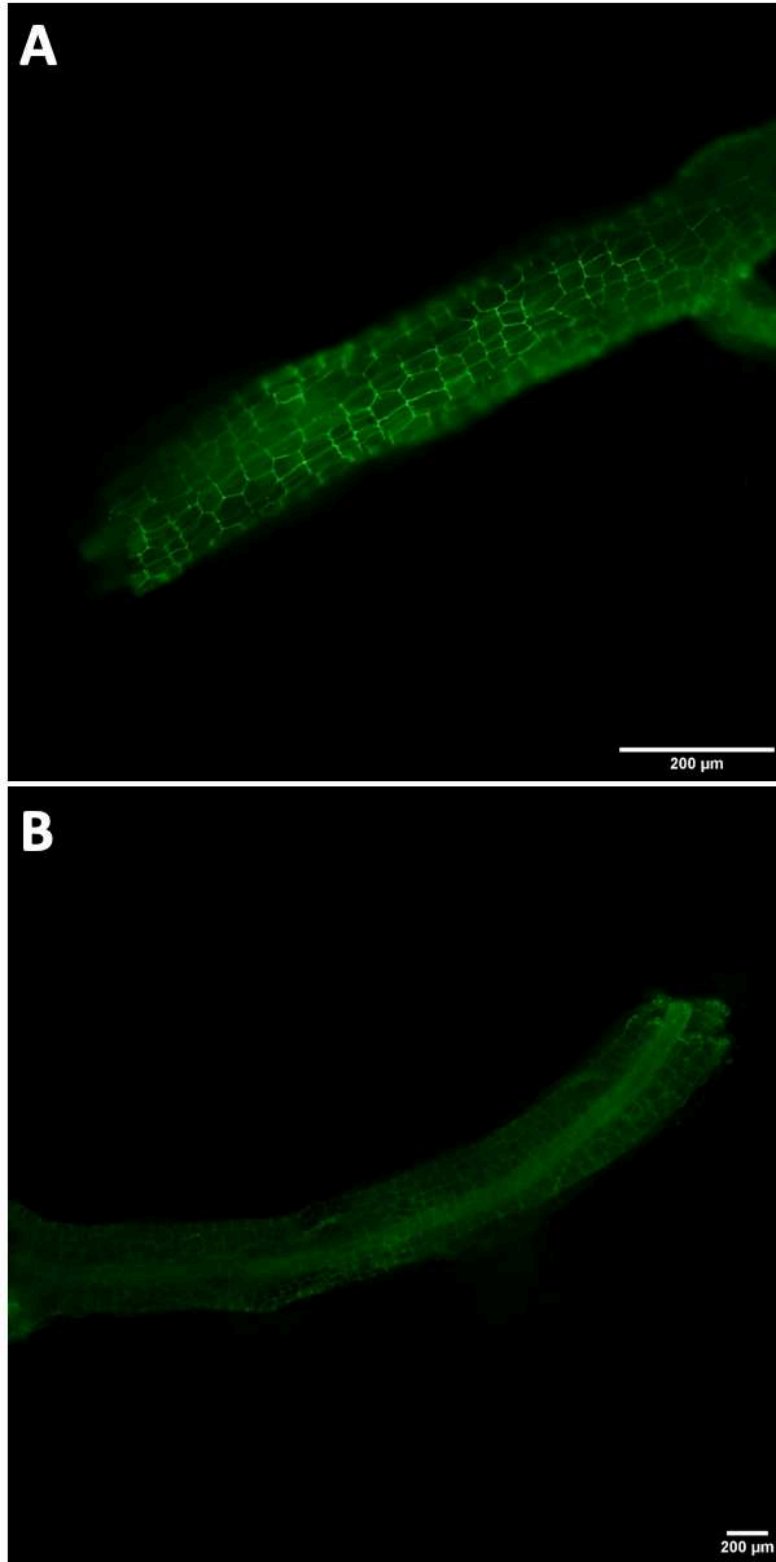
Figure 3.04 Root to shoot transition zone with Fluorol Yellow staining of **A.** Col-0 and **B.** NTB092. Scale bars are 200μm.
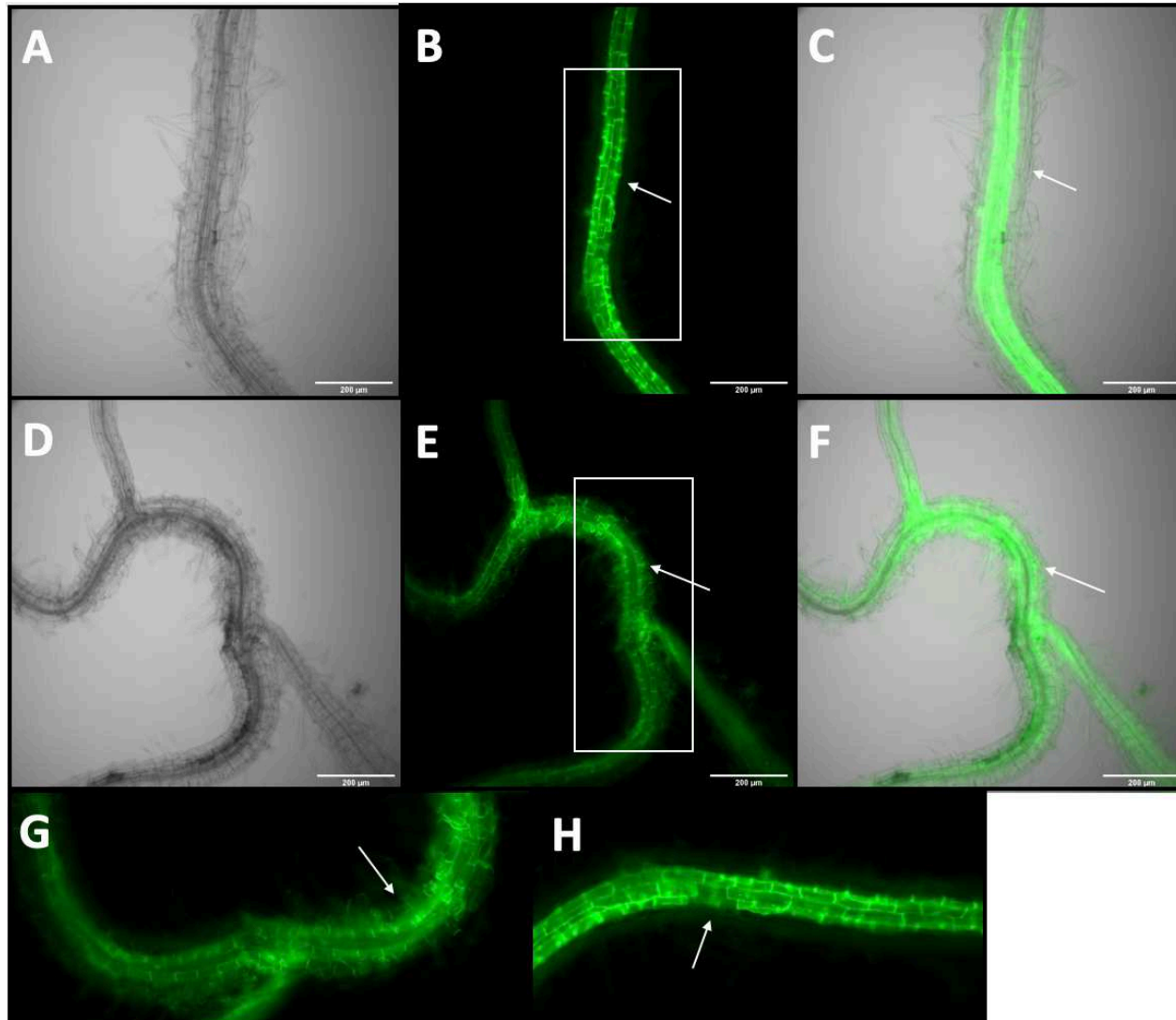
Figure 3.05 Epidermal expression of MYB92 in the maturation zone of 10-day old seedlings. Scale bars are 200μm. **A.** Bright-field Col-0. **B.** Fluorol Yellow stain Col-0. Arrow indicates lack of epidermal suberin. **C.** Merge of panels A and B. Arrow indicating lack of epidermal suberin. **D.** Bright-field NTB092. **E.** Fluorol Yellow stain NTB092. Arrow pointing to suberized epidermal cells with

suberized root hairs. **F.** Merge of panels D and E. Arrow indicating presence of epidermal suberin. **G)** Zoom of white box in panel E. Arrow pointing to suberized epidermal cells. **H.** Zoom of white box in panel B. Arrow indicating lack of suberin in epidermal cells.
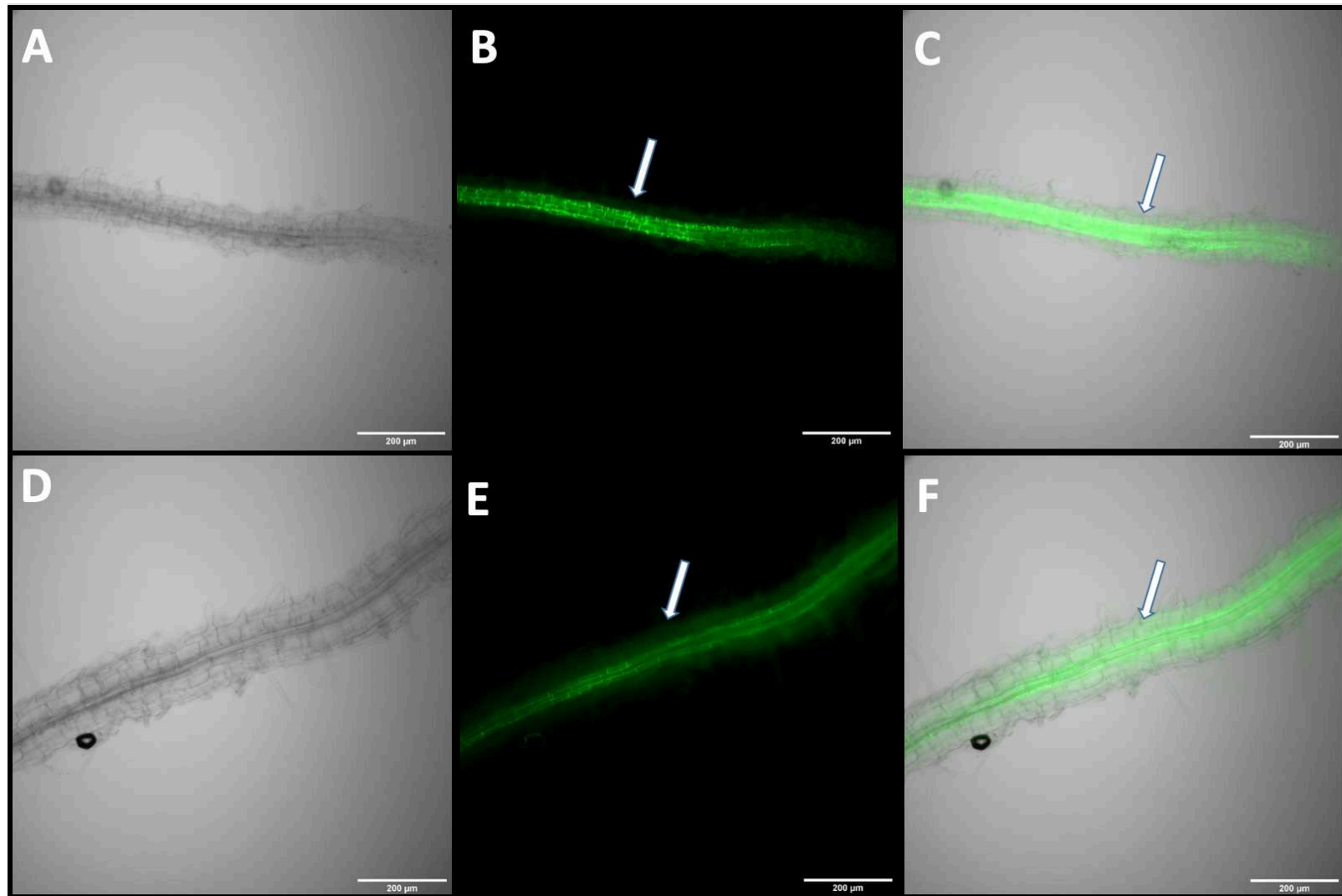
**Figure 3.06** Epidermal expression of MYB92 in the root elongation zone of 10-day old seedlings. Scale bars are 200μm. White arrows indicate lack of epidermal suberin in both Col-0 (**A-C**) and NTB092 (**D-F**). **A.** Bright-field Col-0. **B.** Fluorol Yellow stain Col-0. **C.** Merge of panels A and B. **D.** Bright-field NTB092. **E.** Fluorol Yellow stain NTB092. **F.** Merge of panels E and F.
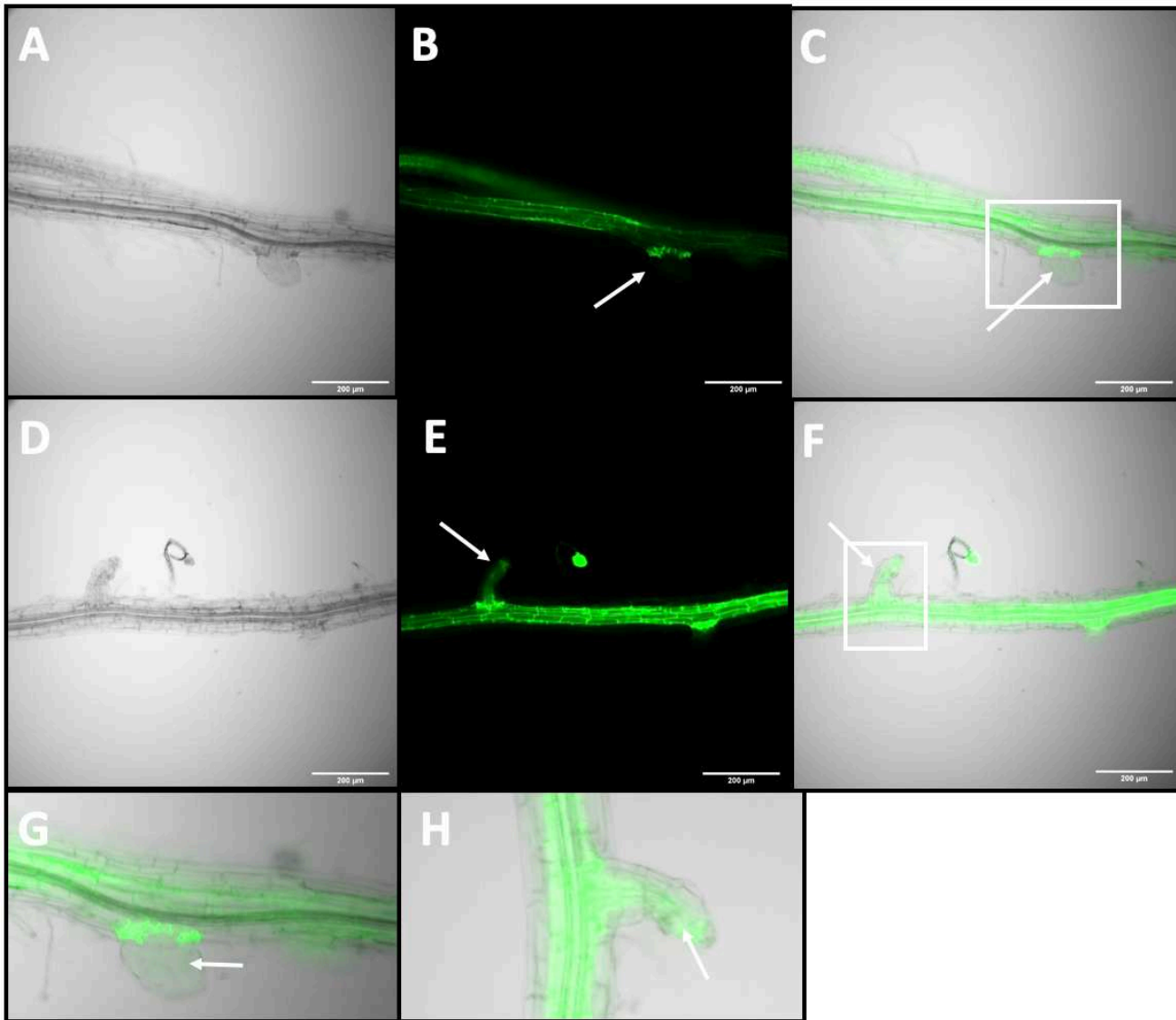
Figure 3.07 Expression of epidermal MYB92 in emerging lateral roots of 10-day old seedlings. Scale bars are 200μm. Image is adjusted for brightness and contrast. **A-C** Col-0; **D-F** MYB92. **A.** Bright-field Col-0. **B.** Fluorol Yellow stain Col-0. Arrow indicates

lack of suberin. **C.** Merge of panels A and B. Arrow indicating lack of suberin. **D.** Bright-field NTB092. **E.** Fluorol Yellow stain NTB092. Arrow pointing to suberin. **F.** Merge of panels D and E. Arrow indicating presence of suberin. **G.** Zoom of white box in panel C. Arrow indicating lack suberized cells. **H.** Zoom of white box in panel F. Arrow indicating suberin.
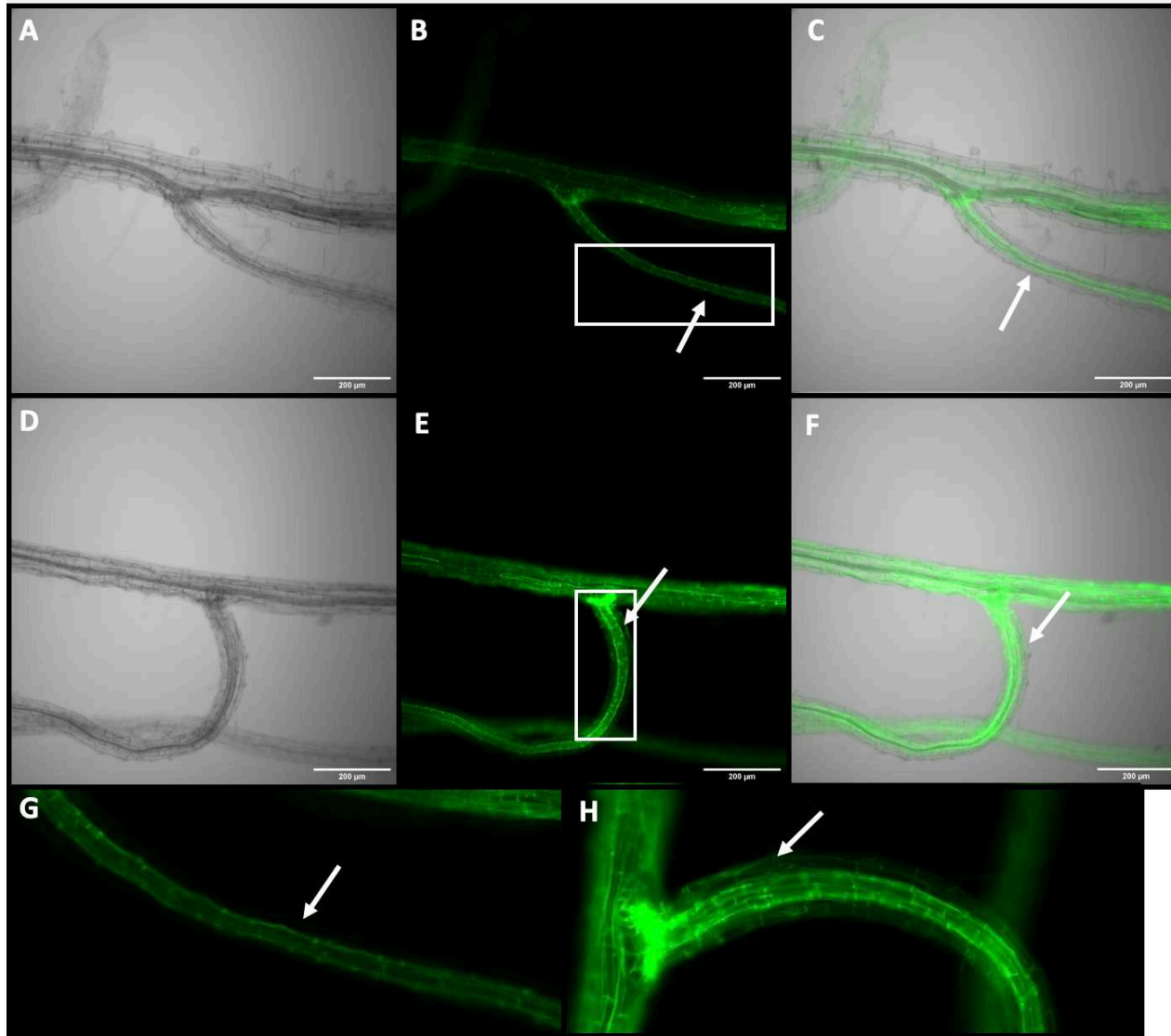
Figure 3.08 Mature lateral roots expressing MYB92 in the root epidermis from 10-day old seedlings. Scale bars are 200μm. **A-C** Col-0; **D-F** NTB092. **A.** Bright-field Col-0. **B.** Fluorol Yellow stain Col-0. Arrow indicates lack of epidermal suberin. **C.** Merge of panels

A and B. Arrow indicating lack of epidermal suberin. **D.** Bright-field NTB092. **E.** Fluorol Yellow stain NTB092. Arrow pointing to epidermal suberin. **F.** Merge of panels D and E. Arrow indicating presence of suberin. **G.** Zoom of white box in panel B. Arrow indicating lack suberized cells. **H.** Zoom of white box in panel H. Arrow indicating epidermal suberin.
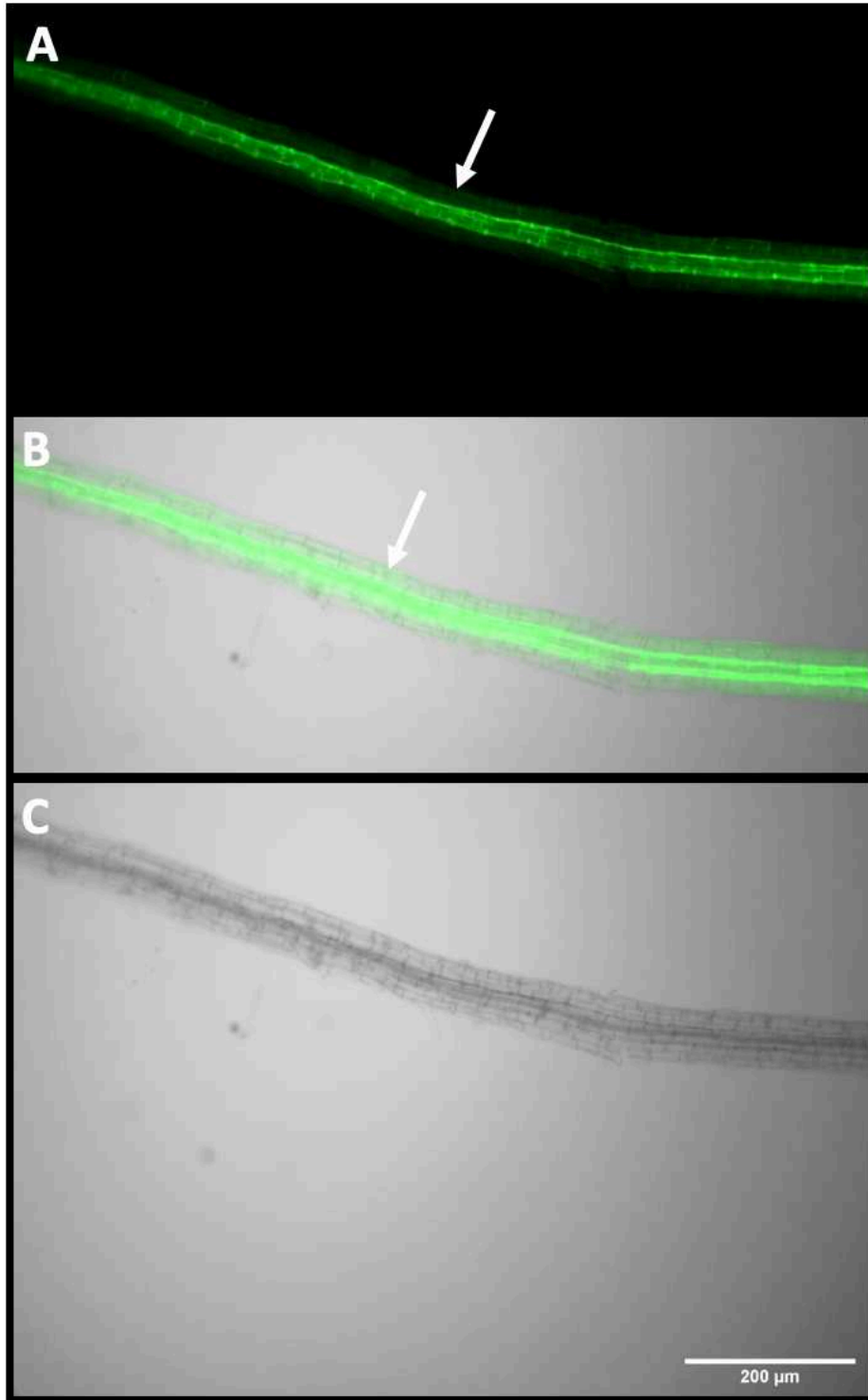
Figure 3.09 – A NTB092 mature lateral root showing suberin in root epidermis. Image adjusted for brightness. White arrows indicate epidermal suberin **A**) Fluorol Yellow stain; **B**) fluorescent and bright field merge; **C**) bright field.
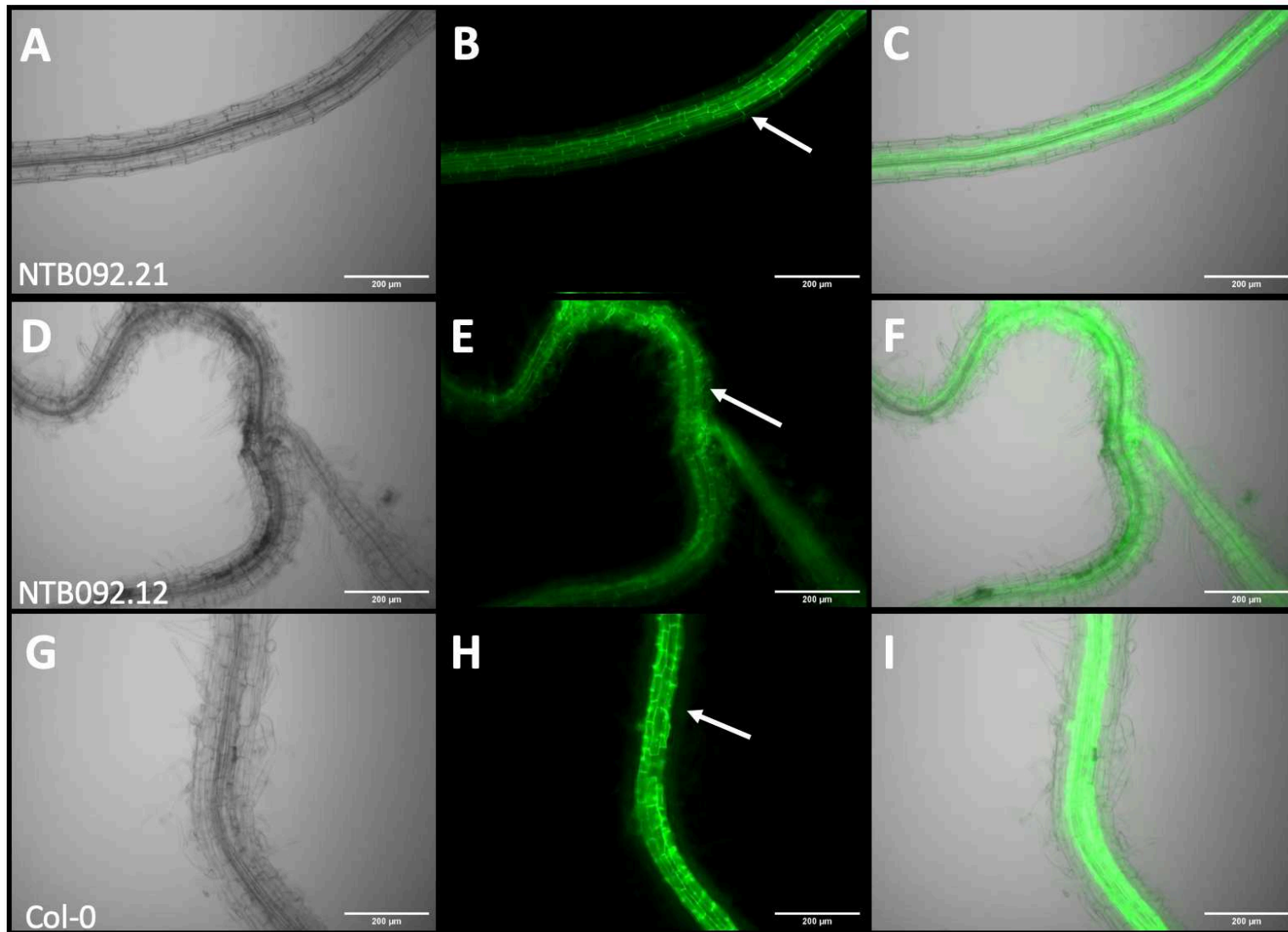
Figure 3.10 Comparison of two independent homozygous lines of NTB092. Scale bars are 200μm. Top: NTB092.21 **A)** bright-field; **B)** Fluorol Yellow stain; **C)** Merge. Arrow pointing to epidermal suberin. Middle: NTB092.12 **D)** bright-field; **E)** Fluorol Yellow

stain; **F)** Merge. Arrow pointing to epidermal suberin. Bottom: Col-0 **G)** bright-field; **H)** Fluorol Yellow stain; **I)** Merge. Arrow indicating lack of epidermal suberin.

3.3 Measurement of root length

Root lengths of WT Col-0 and homozygous transgenic line NTB092 expressing MYB92 and in the root epidermis, was measured in millimeters to determine if roots from NTB092 plants were stunted relative to roots of Col-0 plants. The transgenic line of MYB92 showed significantly shorter root length on average relative to Col-0 (Fig. 3.11). MYB92 roots were about 20 mm shorter on average compared to Col-0 roots.
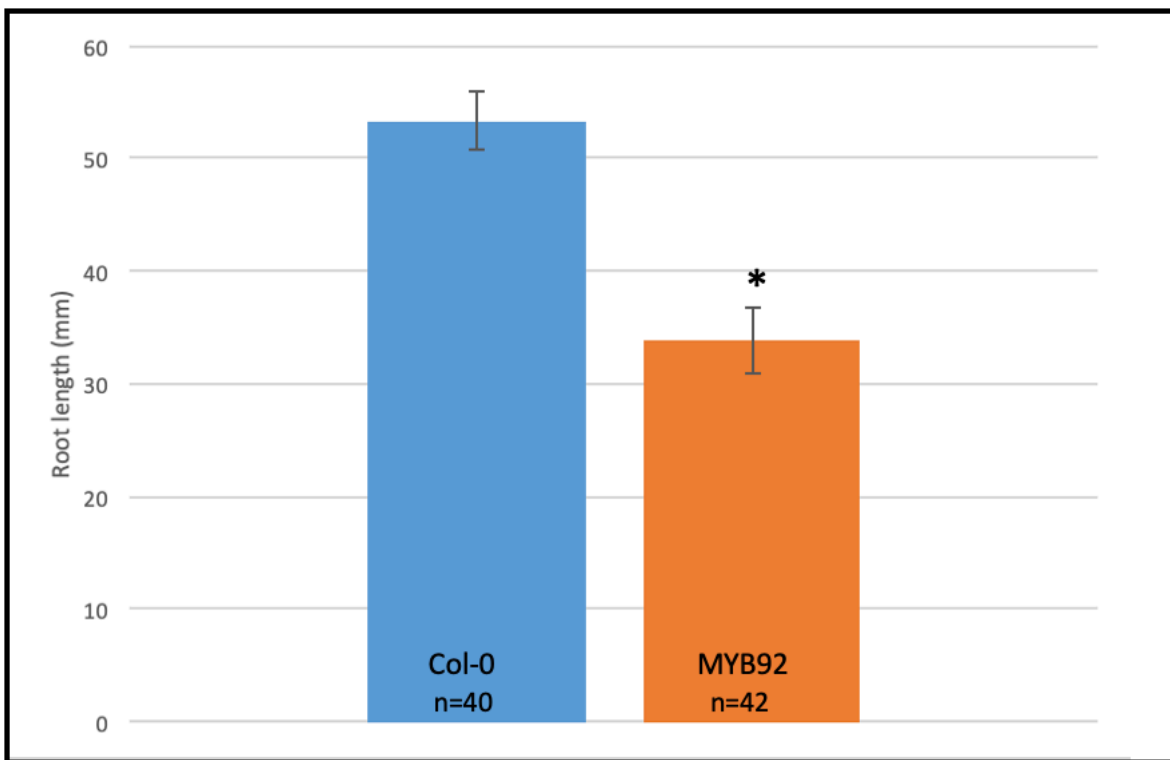

Figure 3.11 Average root length (mm) of Col-0 and NTB092 (MYB92). Error bars are standard error. Col-0 SE=2.53 mm, MYB92 SE=2.91 mm. * denotes significance according to Student's T-test. MYB92 *p=1.47x10^{-5}*.

3.4 RT-qPCR of suberin biosynthesis genes

RT-qPCR was performed in order to determine if suberin biosynthesis genes in the NTB092 line were upregulated compared to suberin biosynthesis genes in Col-0. The biosynthesis pathway was broken down into four stages: aliphatic monomer synthesis (KCS2), aromatic monomer synthesis (FACT), monomer transport (ABCG6), and polymerization (GELP51). One gene involved in each stage, listed prior, was selected to be assayed. In the NTB092 line, all four genes assayed were upregulated. Fatty alcohol caffeoyl-CoA caffeoyl transferase (FACT) was the most upregulated, a 3.78-fold change relative to Col-0 (fig. 3.12d). ABC transporter G family member 6 (ABCG6), 3-ketoacyl-CoA synthase 2 (KCS2), and GDSL-motif esterase/acyltransferase/lipase 51 (GELP51) were all upregulated by about 2-fold change in NTB092 relative to Col-0, 1.97, 2.21, and 1.94, respectively (fig. 3.12).

Table 3.3 – Efficiencies of RT-qPCR primers

Gene	Primer pair efficiency
ACT2	96.5%
KCS2	106.8%
FACT	94.7%
ABCG6	98.6%
GELP51	101.3%
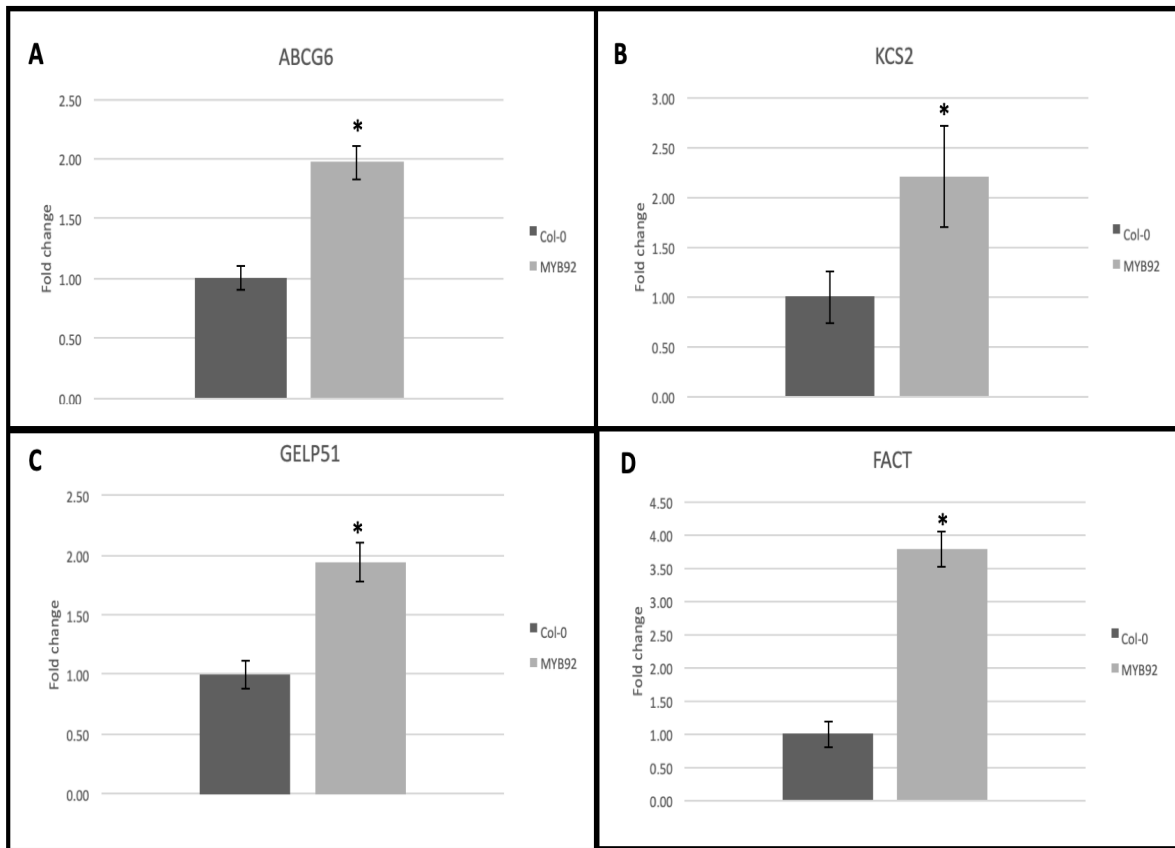
Figure 3.12 – Fold changes of suberin biosynthetic genes in NTB092 plants relative to Col-0. Error bars show standard deviation of fold change values (n=3). * denotes significance of dataset according to student's T-test (*p<0.05*). **A**) ABCG6: *p=6.1x10^{-3}*; **B**) KCS2: *p=0.04*; **C**) GELP51: *p=2x10^{-3}*; **D**) FACT: *p=2.3x10^{-4}*.

3.5 ABA and ACC treatment of Col-0 and NTB092 seedlings

Col-0 and NTB092 were treated with either ABA or ACC by placing plants on media containing either hormone for 24 or 48 hours respectively. Analysis of the roots was qualitative, based on comparison of FY signal strength at equal laser intensity and camera exposure, however, the signal was not quantified. It was expected in both groups of plants that suberization in the endodermis should be increased in response to ABA and that suberization in the endodermis should be decreased in response to treatment with ACC based on published reports

(Barberon 2016). The effect of ABA or ACC treatment on ectopic, epidermal suberin in NTB092 roots was unknown, however, I hypothesized that it would be be similar to that on suberin in endodermis.

Figure 3.13 shows plants with and without ABA treatment. In plants treated with ABA, FY signal does appear throughout the endodermis and is more intense relative to untreated plants (fig. 3.13b,d). Due to the intense strength of FY signal from the endodermis, the relative change between FY signal in ABA treated roots and non-treated roots in the epidermis is hard to characterize (fig. 3.13c,d). Slight variation in FY signal could also have occurred due to the inherent degree of error in the FY staining process making it more difficult to determine subtle differences.
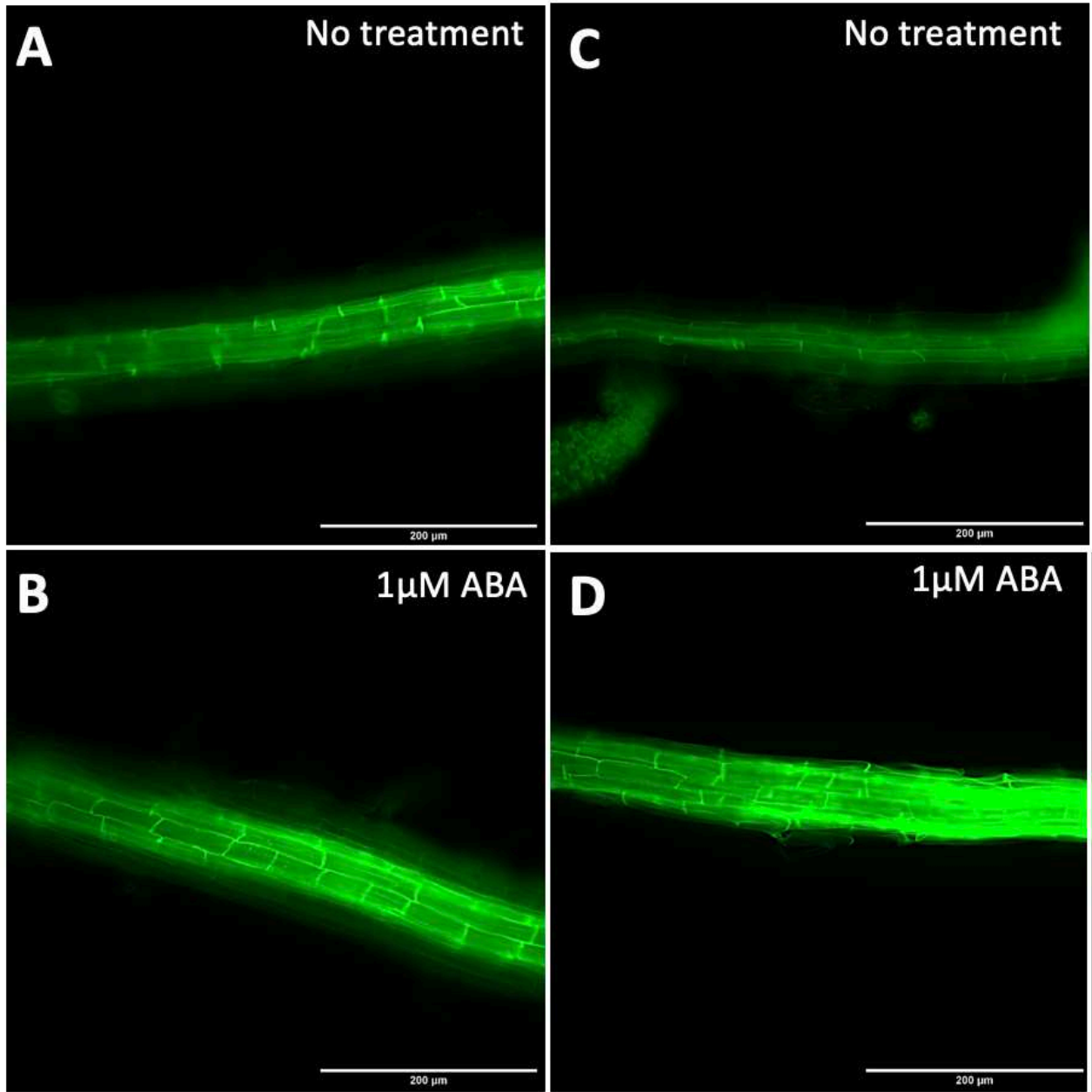
Figure 3.13 ABA treatment of NTB092 and Col-0 roots. Scale bars are 200μm. Image is adjusted for brightness and contrast. **A.** and **B.** Col-0 before and after 24-hour treatment. **C.** and **D.** NTB092 before and after 24-hour treatment.

In plants treated with ACC, the precursor of ethylene, FY signal is diminished post-treatment. In Col-0 (fig. 3.14) and NTB092 (fig. 3.15), FY signal in the endodermis is both less intense and less continuous following ACC treatment. Following treatment endodermal cells show a patchy signal and cell junctions are less defined via fluorescent microscopy suggesting a reduction in suberin in the endodermis (fig. 3.14 and 3.15). Additionally, in plants treated with ACC the endodermis becomes patchy (lacking continuous FY signal) in a more proximal region of the maturation zone compared to untreated plants.

Epidermal suberin in NTB092 plants is reduced to a similar degree as that of the endodermis (fig. 3.15). In some cases it appears that epidermal suberin is completely reduced following ACC treatment, however, this may be slightly affected by the low intensity of FY signal from epidermal suberin relative to the signal from the endodermis. Slight variation in FY signal due to the staining process may also have affected this experiment, however, it was easier to compare the reduction of FY signal in ACC treated roots due to the patchy appearance the FY signal takes on (fig. 3.14a,b; fig. 3.15a,b) than it was to compare a slight increase in signal in the ABA treated roots (fig. 3.14).
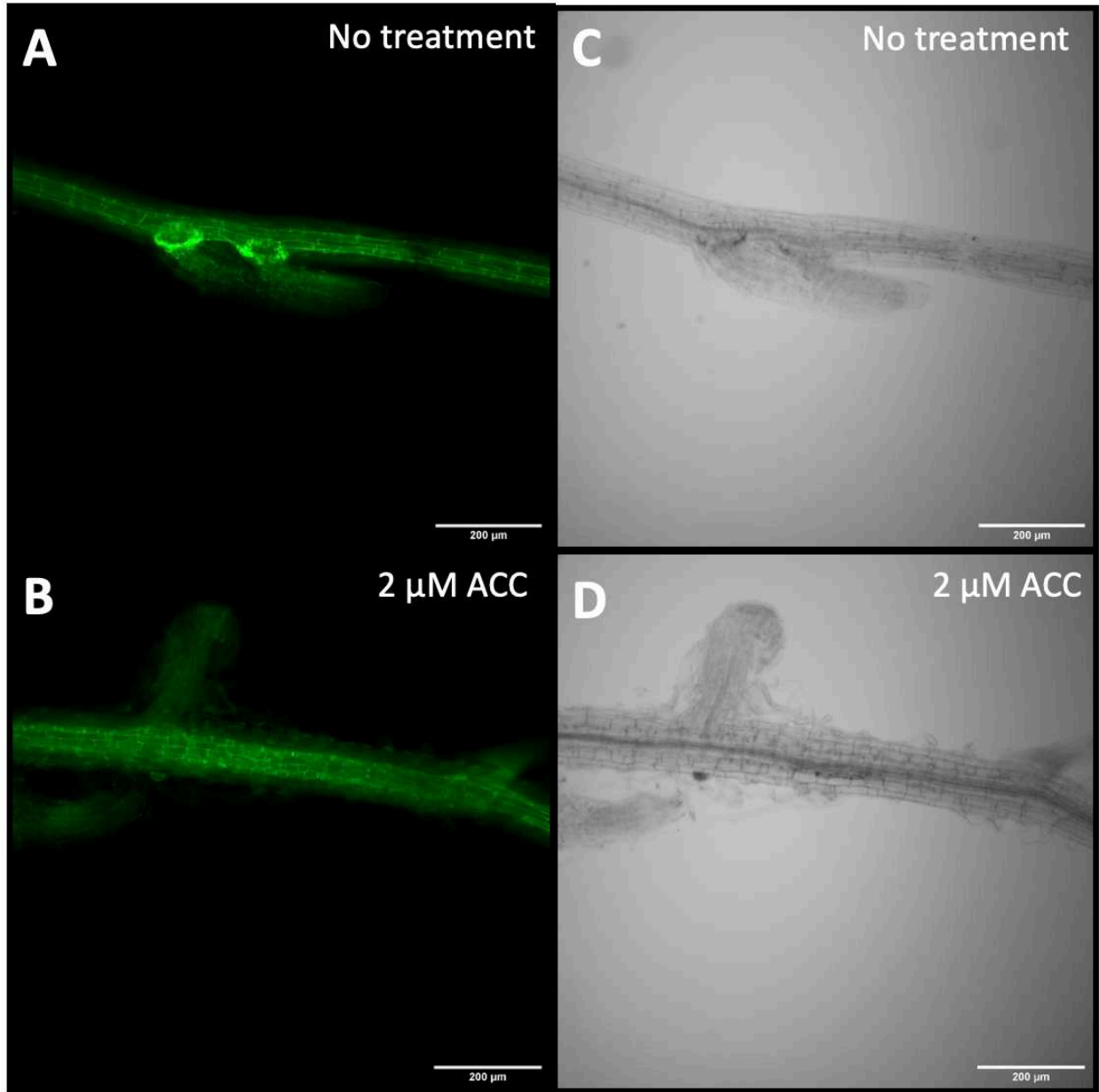
Figure 3.14 ACC treatment of Col-0 10-day old roots. Scale bars are 200µm. Panels **A** and **C** show untreated Col-0 roots. Panels **B** and **D** show Col-0 roots following 48-hour ACC treatment.
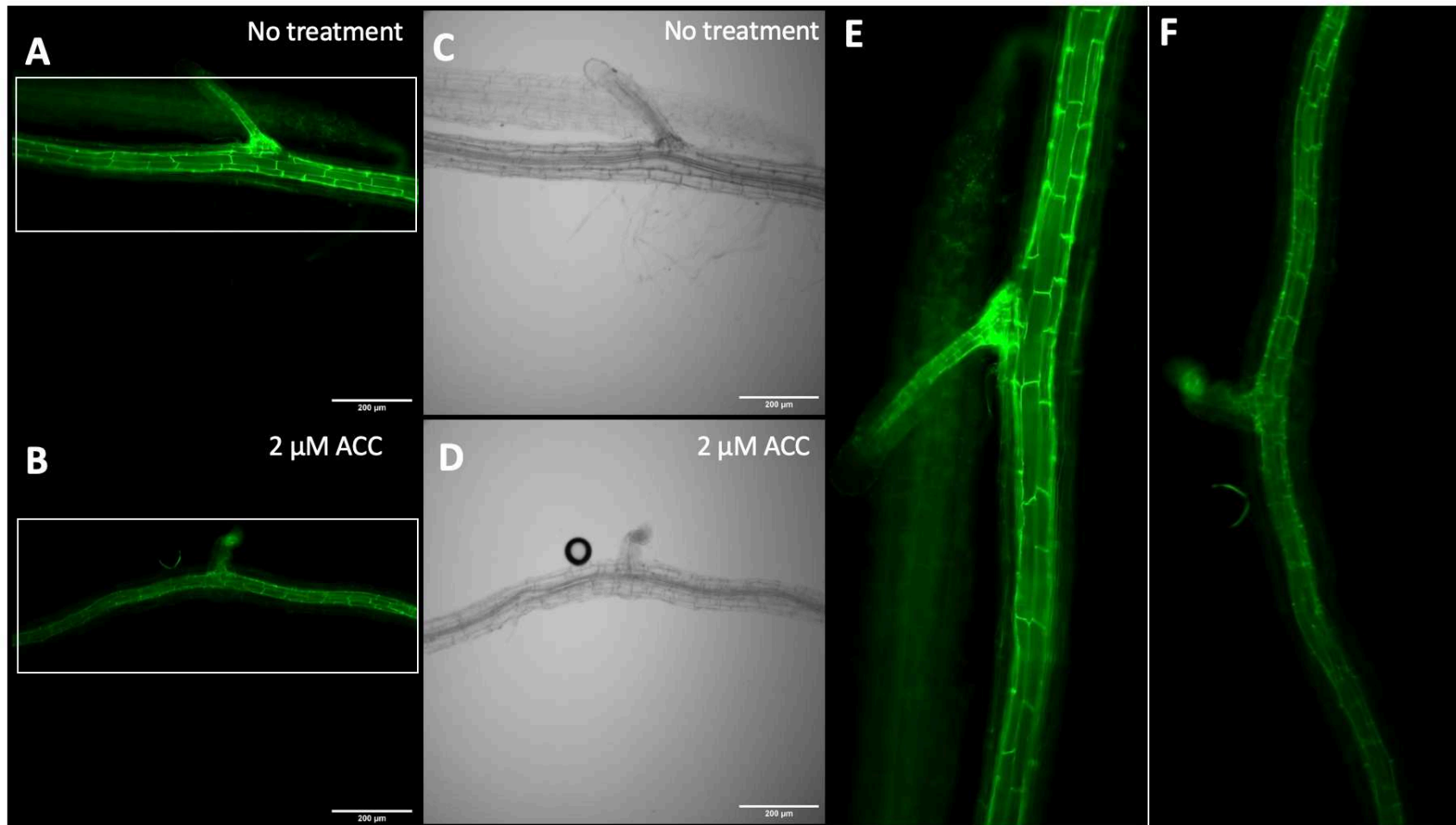
Figure 3.15 ACC treatment of NTB092 10-day old roots. Scale bars are 200μm. Panels **A** and **C** show untreated Col-0 roots. Panels **B** and **D** show NTB092 roots following 48-hour ACC treatment. **E.** Zoom of panel A. **F.** Zoom of panel B.

3.6 Sodium chloride treatment of transgenic and wild type plants

Mature Col-0 (n=8) and NTB092 (n=9) plants were treated with 50 mM NaCl for seven days. Following treatment, Col-0 plants show chlorosis and anthocyanin accumulation in their rosettes (fig. 3.16). NTB092 plants, following treatment do not show any chlorosis or anthocyanin accumulation (fig. 3.16).
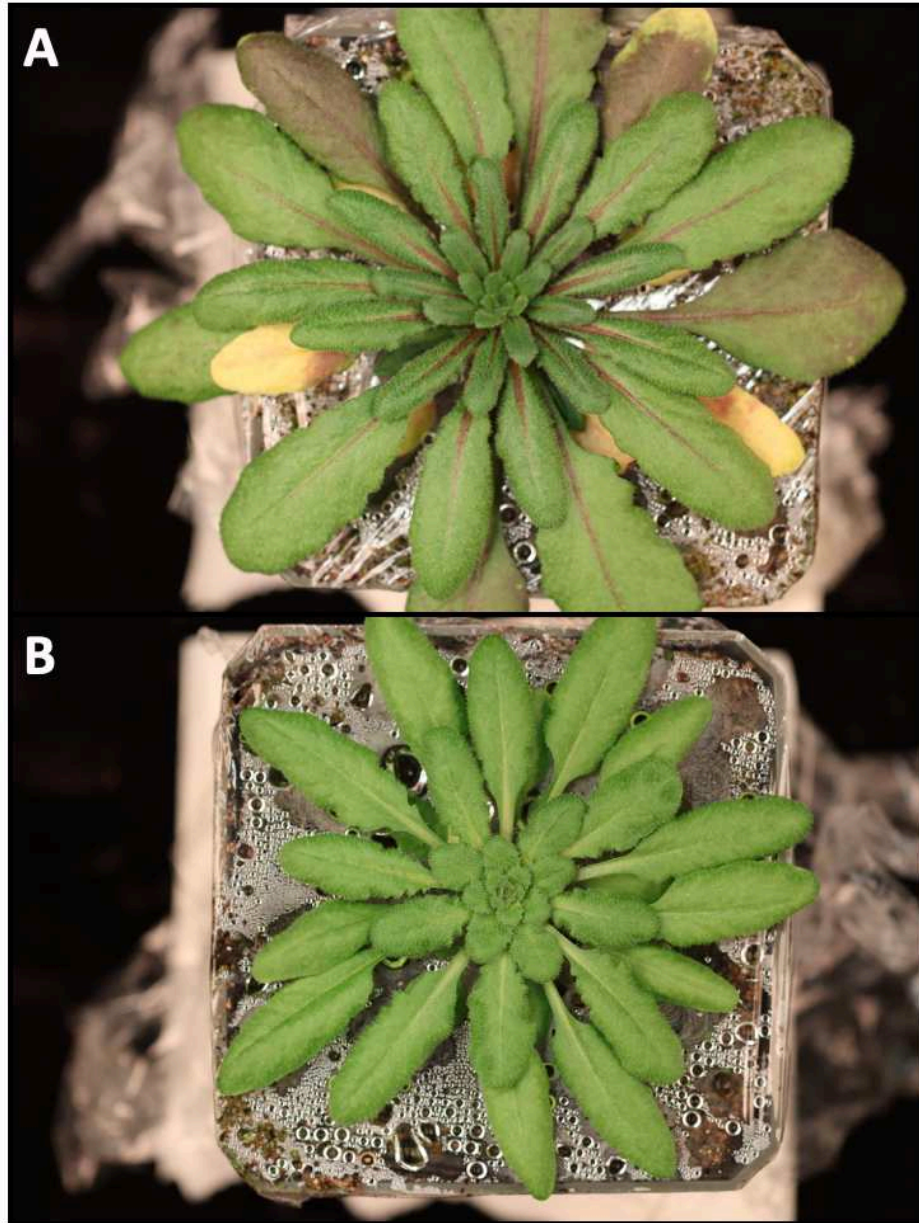
Figure 3.16 NTB092 plant showing salt-tolerance. Plants were treated for seven days with 50mM sodium chloride. **A.** Col-0 plant with chlorosis and anthocyanin accumulation in lower rosette. A hallmark of salt stress. **B.** NTB092 plant exhibiting minimal stress.

Chapter Four: Discussion

The results described in my thesis characterize the ability of a specific group of R2R3-MYB transcription factor's ability to ectopically induce the biosynthesis of suberin. Some of these genes have been demonstrated to be involved in the activation of suberin biosynthesis via gene knock out experiments: MYB9, MYB92, MYB93 (Lashbrooke et al. 2016; Shukla et al. 2021). MYB67, the other gene tested in this work, has been predicted *in silico* to be involved in suberin biosynthesis and has been shown to be upregulated in cork tissues via transcriptomics data (Czechowski et al. 2004; Rains et al. 2018). Expression of these genes was specifically targeted to the root epidermis by cloning the genes into an expression vector placing them under control of the ABCG37 promoter. The ABCG37 gene encodes a protein involved in root exudation (Ziegler et al. 2017) and its promoter drives expression solely in the root epidermis (Oehmke 2020).

Of the genes tested, only MYB92, when expressed in the root epidermis, consistently showed roots which contained a suberized epidermal layer (fig. 3.10). Five potential reasons for the inability of the other MYB genes to induce ectopic suberization may be 1) the tested MYB gene simply is not involved in suberin formation, 2) lack of proper post-translational modification which is required to activate the MYB gene, 3) the MYB gene is involved in suberin formation, but not in a tissue of the root, and lacks the necessary regulatory elements for its expression, 4) there is a repressor of the transcription factor which is expressed in the root epidermis, or 5) epigenetic silencing of the T-DNA insertion following transformation. Initially, I thought that epigenetic silencing was occurring, however, this was determined to not be the

case based on the measured segregation of the kanamycin resistance transgene in all of the lines analyzed (Table 3.2).

One issue that was encountered during the screening process was that of false positive screens. The Fluorol Yellow 088 stain may partially stain lipids other than suberin, and suberin is not the only lipid found in the apoplast, so it was therefore difficult in some cases to determine if the FY signal was entirely coming from suberin. Following a second round of screening independent lines, establishment of two homozygous lines, and then rescreening heterozygous plants of one of those lines, I determined that many of the initial positive screens for epidermal suberin in plants containing the NTB093 construct were actually false positives. The preliminary screening described in this thesis was done using a Leica DFC450 microscope camera, whereas the secondary screening and characterization was done using a Leica K5 microscope camera. The DFC540 camera is an all-purpose microscope camera whereas the K5 camera is specialized for fluorescent microscopy, the main technique used in my thesis. In addition, the K5 camera is several years more modern than the DFC450. The K5 camera enabled much more meticulous detection of the FY stain signal, making it easier to determine which samples were false positives. Transgenic lines, stained with FY stain and viewed under the DFC450 camera show blue signal at cell wall junctions in the root epidermis even though there may not be suberin in that location. I initially could not determine if the blue signal was from suberin or due to the DFC450 camera. The same lines show no FY signal in those locations when viewed under the K5 microscope, making the K5 camera superior for detecting suberin in the root epidermis. After viewing transgenic lines stained with FY under the K5 camera, I concluded the blue signal was not from suberin or FY stain. RT-qPCR was performed on plants containing the NTB092

construct and showed that several suberin biosynthesis genes were upregulated in roots of plants from this line, confirming that the FY signal in these plants was a true signal (fig. 3.12).

A second issue regarding the FY stain is the variation between samples, inherent to the use of this stain. The stain must be washed with three rinses with water before mounting in 50% glycerol. Because the FY stain can only be removed and replaced with water in one root sample at a time, some roots end up being stained and washed for slightly longer than others. The greater number of samples one is working with, the more severe this problem will become. Although I initially believed the variation in FY signal between roots within the same NTB092 line was due to epigenetic silencing, I now conclude that this variation was likely due to error in the staining process.

MYB9, MYB67, and MYB93 all failed to consistently induce epidermal suberin formation. A possibility for the ineffectiveness of MYB9, MYB67, and MYB93 to induce epidermal suberization may be a lack of a proper post-translational modification. MYB41, which has been shown to control suberin biosynthesis to some degree, requires a phosphorylation by mitogen-activated protein kinase 6 (MPK6) at serine 251 in order to induce salt tolerance in plants which overexpress it (Hoang 2012). The proteins which regulate MYB9, MYB67, and MYB93 are unknown, and no data has been published on sites of post-translational modifications for these proteins either. In this study *in silico* tools were used to predict phosphorylation sites of which each MYB transcription factor showed multiple amino acid residues which were strong candidates for phosphorylation. The nature of the regulation of the MYB genes in this study could be characterized similarly to Hoang et al. 2012's characterization of MYB41. This characterization must take place both *in vitro* and *in planta* due to the fact that *in vitro* protein interaction assays do not account for specific plant physiological processes.

One way in which this issue of post-translational modification has been overcome is by the use of phosphomimetry. An engineered MYB41 containing an aspartic acid residue at position 251 rather than a serine is able to mimic the effect of phosphorylation and is able to induce suberization in the root epidermis (Medford et al. 2020). Based on this, four phosphomimetic MYB proteins were made my study. The residues chosen to be engineered were based on sequence homology to MYB41, as well as *in silico* predictions of phosphorylation sites on MYB67 and MYB102. The engineered MYB102 proteins were not successfully able to be transformed into plants, and I suggested that this gene may be lethal to the plant when ectopically expressed (table 3.1). The engineered MYB67 proteins were successfully transformed into plants, however, there was no difference in phenotype when compared to the non-engineered MYB67 construct (table 3.1). It may be that the wrong residue was mutated, i.e., the protein is phosphorylated in a different location or requires multiple sites of phosphorylation or that the phosphomimic was simply ineffective. In a future experiment an engineered MYB67 protein containing both the modified threonine and serine residues tested in this study may yield a better result if the protein does in fact require more than one phosphorylation in order to be activated.

A third possibility for the failure of the MYB genes to induce suberin biosynthesis is that they simply are not involved in regulating suberin biosynthesis. A quad mutant lacking functional MYB41, MYB53, MYB92, and MYB93 exhibits impaired suberin formation in its endodermis (Shukla et al. 2021), however, the individual contributions of each of these genes to suberin biosynthesis is not understood. Results from my work indicate that MYB92 is involved in regulating suberin biosynthesis. Whether or not MYB93 is actually involved in regulating suberin biosynthesis is unknown. MYB67 is predicted *in silico* to be involved in suberin

formation and is demonstrated to be upregulated in cork tissue via transcriptomic analysis

(Czechowski et al. 2004; Rains et al. 2018), however, there is no direct evidence that MYB67 is

involved in regulating suberin biosynthesis.

A fourth possibility for the failure of the MYB genes to induce suberin biosynthesis in

the root epidermis is that the gene is involved in suberin biosynthesis, but is endogenously

expressed in a tissue other than the endodermis, such as the seed coat. MYB9 likely is involved

in suberin biosynthesis as *Arabidopsis* mutants which lack a functional copy of the gene exhibit a

significant reduction of suberin monomers in their seed coats (Lashbrooke et al. 2016). Since

MYB9 appears to regulate suberin in the seed coat rather than the endodermis, there could be a

difference in the way the gene is regulated compared to MYB genes expressed in the endodermis

which would need to be accounted for to express the gene in the root. MYB9 contained no highly

predicted phosphorylation sites in its C-terminus region based on *in silico* predictions which

suggests it is activated via a different pathway than MYB41. Since it is unknown which genes

regulate MYB9, there is no way of determining if its regulators are expressed in the root. As

suggested above, protein-protein interaction assays could be valuable to understand the nature of

regulation of these MYB genes.

It may also be the case that rather than the MYB protein requiring a protein to activate it

which is not expressed in the root epidermis, that there is a repressor of the MYB protein which

is expressed in the root epidermis, but not in the endogenous tissue such as cork, the endodermis,

or seed coat. Suberin is deposited in a very tissue-specific and cell-specific manner in the

locations it is found, thus, it may make sense for there to be a common repressor of the proteins

which control its deposition in tissues and cells where suberin is not deposited. If this is the case

the gene responsible for that repressor would need to be identified and its expression reduced

within the root epidermis using RNAi or CRISPR in order to determine if the MYB gene can effectively induce suberin biosynthesis.

The transgenic lines expressing MYB92 in the root epidermis showed consistent biosynthesis of suberin in that area (fig. 3.10). Plants which express MYB92 in the root epidermis, and thus contain a synthetic suberin barrier, are chlorotic and stunted in root and shoot size, particularly when grown on plates with MS media (fig. 3.01,3.02, 3.11). When placed into soil much of the chlorosis recovers and some plants increase growth rate to that similar of Col-0. Interestingly, when treated with 50mM NaCl for 7 days the NTB092 plants show little to no change (fig. 3.16). Col-0 plants following a 50mM NaCl treatment show typical signs of salt stress such as chlorosis and necrosis in bottom of the rosette and anthocyanin accumulation in leaves and petioles consistent with deficiency in potassium and ROS accumulation respectively (fig. 3.16) (Xiong and Zhu 2002). Suberin biosynthesis in known to be induced by NaCl over-accumulation outside the root and by lack of potassium in the root (Barberon 2017). This confers salt tolerance by blocking NaCl from entering the plant and blocking K^+ from leaving the plant. Na^+ accumulation leads to a general reduction in cellular K^+ levels leading to chlorosis, necrosis and decreased turgor (Xiong and Zhu 2002). In this study, the additional suberin barrier in the root epidermis is likely having an additive effect with that of the endodermis, further working to keep NaCl outside of root cells and K^+ ions inside of root cells.

My work noted that the pattern of suberization in the epidermis is variable both within a single root and between roots of different plants. Within a single taproot of NTB092 plants there are areas of dense, continuous suberin in the epidermis, areas of patchy suberized cells, and areas of little to no suberized cells. Lateral roots exhibit little variation in their degree of suberized cells (fig. 3.07; 3.08; 3.09). The lateral roots exhibit consistent, and continuous suberin from the

base of the root emergence to the root elongation zone. Compared to suberin in the endodermis, the FY signal is almost always weaker in the epidermis (fig. 3.10). A possible reason for this is that the combination of multiple endogenous transcription factors controlling suberin biosynthesis (Shukla et al. 2021) results in a greater, and more consistent degree of suberin in endodermal cells when compared to a single transcription factor, expressed ectopically in the root epidermis. As more controllers of suberin biosynthesis are identified it would be judicious to experiment with expressing combinations of them in the root epidermis. It may be possible, with a combination of transcription factors to achieve a barrier with a similar degree, consistency, and continuity as that of the endodermis. This, in turn, may confer an even greater abiotic stress tolerance to plants containing this barrier.

After performing RT-qPCR, I found that the four genes assayed were upregulated between 1.94 and 3.78 fold-change (fig. 3.12). The suberin biosynthesis pathway can be roughly broken down into four phases: synthesis of the aliphatic monomers, synthesis of the aromatic monomers, transport of those monomers to the cell wall, and polymerization of those monomers/oligomers at the cell wall. The genes chosen to represent those pieces were KCS2, FACT, ABCG6, and GELP51 respectively. There are many more genes involved in the biosynthesis pathway of suberin and a more comprehensive RT-qPCR assay could be carried out in the future in order to better understand the suberin composition being synthesized in the root epidermis. Furthermore, chromatography-mass spectroscopy could be carried out on an extraction of the epidermal lipids in the root to get a true picture of the difference in composition and quantity of suberin in NTB092 roots versus Col-0 roots. It will be interesting to determine if enzymes involved in this pathway can become more upregulated by co-expressing multiple MYB transcription factors in the root epidermis.

On a similar note, it would be interesting to use an RT-qPCR assay in order to characterize the biosynthesis response following treatment with ABA or ACC (ethylene). This study features a qualitative characterization, using fluorescence microscopy, of this response, however this could be quantitative in the future. From initial results found in this study, it appears that epidermal suberin is subject to similar regulation by ACC as that of suberin in the endodermis i.e., suberization is decreased in response to ethylene (ACC) (fig. 3.14; 3.15) (Barberon 2016). The response to ABA within the epidermis was challenging to analyze qualitatively due to the overwhelming amount of FY signal which comes from the endodermis (fig. 3.13). The large amount of FY signal, consistently found in the endodermis, makes it challenging to judge minute increases in FY signal in the epidermis. This could potentially be remedied using confocal microscopy, however, I expect that FY signal from the endodermis would still confer a degree of difficulty in the study. Looking forward, a future study could use RT-qPCR in order to establish a curve of timing in respect to the upregulation or downregulation of the suberin biosynthesis genes. This RT-qPCR assay could also yield data on the minimum amount of each hormone required for a particular response. This knowledge could be useful to reduce/induce the barrier under particular conditions. This could be valuable, for example, in crops where a barrier could be induced prior to a drought, and then reduced after to switch the root back to an absorbent state.

Other inducible gene expression systems which have been characterized in plants may complement the NTB092 construct as well. One such system that could potentially be adapted to synthetic barriers is a stress-induction system. The promoter of heat shock protein 18.2 (HSP18.2) from *Arabidopsis* has been demonstrated to activate transgenes following heat shock at 37°C. Building on this, Harrington et al. 2020 created a heat shock inducible system for cereal

crops which can drive constitutive gene expression of a gene of interest indefinitely following heat shock. Their system is Cre recombinase based where the inducible promoter drives expression of the recombinase which is targeted to a second construct containing a constitutive promoter followed by a reporter, followed by a gene of interest. Induction of the stress promoter leads to recombination in the second construct placing the gene of interest under control of the constitutive promoter and excising the reporter (Harrington et al. 2020). This system could potentially be modified to be tissue specific provided that the stress induced promoter is expressed in the desired tissue and the constitutive promoter was swapped for a tissue specific promoter. If this was done, plants could possibly be generated which lack the additional suberin barrier until responding to a particular stress such as heat or salt. Following the stress, plants could automatically synthesize the barrier with no human intervention, allowing them to subsist longer into a drought or heatwave. Two examples of promoters which could potentially drive this system are the *Arabidopsis* RD29A and RD29B promoters. These promoters have been demonstrated via GUS (β-glucuronidase) fusion to be constitutively induced in response to drought-stress in soybeans (Bihmidine et al. 2013). GUS expression in those transgenic soybeans was higher in the roots compared to the leaves of the plant (Bihmidine et al. 2013) which would benefit a system where the gene of interest was a MYB gene under control of the ABCG37 promoter.

Although this is the first study to characterize MYB92 expression specifically in the root epidermis, studies characterizing MYB92 overexpression mutants have made similar conclusions about the gene's biological function. To et al. 2020 found that, following transient expression of MYB92 with the CaMV dual 35s promoter in *N. benthamiana*, suberin deposition in leaves was increased 50-fold. RT-qPCR data from that study indicated that, in MYB92 overexpressing lines,

NbASFT, NbKCS1, NbCYP86B1, NbGPAT4, and NbGPAT5 were all upregulated (To et al. 2020). These genes are involved in similar processes or are upstream/downstream of the genes assayed by RT-qPCR in this study, which were also upregulated. Interestingly, To et al. 2020 found that C16:0 and C18:1 fatty acids were increased by 223-fold and 152-fold respectively, whereas ferulic acid (an aromatic component of suberin) was increased 17-fold. This furthers the potential value of a chromatography-mass spectroscopy analysis of the root epidermal suberin in this study, to determine if its composition is similar to that formed in the leaf following transient MYB92 expression.

Another group, Shukla et al. 2021, generated a quad-mutant using CRISPR-Cas9 which lacked functional copies of MYB41, MYB53, MYB92, and MYB93. In that mutant, suberin formation in the root was almost entirely impaired, even upon addition of environmental and developmental suberin activators (ABA and CIF2). Similarly, the majority of suberin biosynthesis genes were downregulated in the quad-mutant (Shukla et al. 2021). Certainly, a single mutant, lacking functional MYB92, could be generated to measure the sole effect of MYB92. Likely, in this case the other MYB genes mentioned above will mask the effect of a non-functional MYB92, as was demonstrated with MYB41 (Shukla et al. 2021).

An engineered MYB41 (phosphomimic) has been shown to induce root epidermis specific suberization (Medford et al. 2020). A future study should test the effect of both the engineered MYB41, and MYB92 when expressed simultaneously in the root epidermis. Since suberin formation in the endodermis appears to be controlled by multiple R2R3-MYB transcription factors (Shukla et al. 2021), expression of multiple transcription factors in the epidermis may lead to a higher degree of suberization, more similar to that of the endodermis.

In conclusion, I have shown in this study that MYB92 is capable of inducing suberin biosynthesis in a tissue-specific manner in *Arabidopsis* roots. Expression of MYB92 in the root epidermis leads to increase in expression of various suberin biosynthesis genes, and distinct morphological changes to the cell wall structure of root epidermal cells. In turn, those morphological changes confer a degree of salt-tolerance relative to wild-type plants. The extent of this salt tolerance could be further investigated. The results in this study complement those of Kosma et al. 2014 and To et al. 2020 which investigated the ability of MYB41 and MYB92, respectively, to induce ectopic suberization when the genes are overexpressed. This study further implicates MYB92 as a positive regulator of suberin biosynthesis and provides evidence that the metabolic process of suberin biosynthesis can be compartmentalized and targeted to a specific tissue of the root. Manipulation of suberin barriers in plants may emerge as a practical tool to tailor the input and output of particular ions through plant tissues in order to control plant responses to abiotic stresses such as salt and drought. Further characterization of MYB92 is recommended to entirely understand its role in responding to abiotic stresses and as a controller of suberin biosynthesis.

Literature Cited

Akhtar, S., A. Ahmed, M. A. Randhawa, S. Atukorala, N. Arlappa, T. Ismail, and Z. Ali. 2013. Prevalence of Vitamin A Deficiency in South Asia: Causes, Outcomes, and Possible Remedies. *Journal of Health, Population, and Nutrition* 31: 413–423.

Alassimone, J., S. Naseer, and N. Geldner. 2010. A developmental framework for endodermal differentiation and polarity. *Proceedings of the National Academy of Sciences of the United States of America* 107: 5214–5219.

Aloni, R., D. E. Enstone, and C. A. Peterson. Indirect evidence for bulk water flow in root cortical cell walls of three dicotyledonous species. 7.

Barberon, M. 2017. The endodermis as a checkpoint for nutrients. *New Phytologist* 213: 1604–1610.

Barberon, M., J. E. M. Vermeer, D. De Bellis, P. Wang, S. Naseer, T. G. Andersen, B. M. Humbel, et al. 2016. Adaptation of Root Function by Nutrient-Induced Plasticity of Endodermal Differentiation. *Cell* 164: 447–459.

Batista-Silva, W., P. da Fonseca-Pereira, A. O. Martins, A. Zsögön, A. Nunes-Nesi, and W. L. Araújo. 2020. Engineering Improved Photosynthesis in the Era of Synthetic Biology. *Plant Communications* 1: 100032.

Bihmidine, S., J. Lin, J. M. Stone, T. Awada, J. E. Specht, and T. E. Clemente. 2013. Activity of the Arabidopsis RD29A and RD29B promoter elements in soybean under water stress. *Planta* 237: 55–64.

Bonnett, H. T. 1968. THE ROOT ENDODERMIS: FINE STRUCTURE AND FUNCTION. *The Journal of Cell Biology* 37: 199–205.

Borevitz, J. O., Y. Xia, J. Blount, R. A. Dixon, and C. Lamb. 2000. Activation Tagging Identifies a Conserved MYB Regulator of Phenylpropanoid Biosynthesis. *The Plant Cell* 12: 2383–2393.

Byrne, M. E., R. Barley, M. Curtis, J. M. Arroyo, M. Dunham, A. Hudson, and R. A. Martienssen. 2000. Asymmetric leaves1 mediates leaf patterning and stem cell function in Arabidopsis. *Nature* 408: 967–971.

Cleland, E., I. Chuine, A. Menzel, H. Mooney, and M. Schwartz. 2007. Shifting plant phenology in response to global change. *Trends in Ecology & Evolution* 22: 357–365.

Compagnon, V., P. Diehl, I. Benveniste, D. Meyer, H. Schaller, L. Schreiber, R. Franke, and F. Pinot. 2009. CYP86B1 Is Required for Very Long Chain ω -Hydroxyacid and α , ω -

Dicarboxylic Acid Synthesis in Root and Seed Suberin Polyester. *Plant Physiology* 150: 1831–1843.

Coudert, Y., Perin, C. Courtois, B. et al. 2010. Genetic control of root development in rice, the model cereal. *Trends in plant science*. 15: 219-226.

Czechowski, T., R. P. Bari, M. Stitt, W.-R. Scheible, and M. K. Udvardi. 2004. Real-time RT-PCR profiling of over 1400 Arabidopsis transcription factors: unprecedented sensitivity reveals novel root- and shoot-specific genes. *The Plant Journal* 38: 366–379.

Doblas, V. G., N. Geldner, and M. Barberon. 2017. The endodermis, a tightly controlled barrier for nutrients. *Current Opinion in Plant Biology* 39: 136–143.

Dolan, L., K. Janmaat, V. Willemsen, P. Linstead, S. Poethig, K. Roberts, and B. Scheres. 1993. Cellular organisation of the Arabidopsis thaliana root. *Development* 119: 71–84.

Domergue, F., and D. K. Kosma. 2017. Occurrence and Biosynthesis of Alkyl Hydroxycinnamates in Plant Lipid Barriers. *Plants* 6.

Du, H., B.-R. Feng, S.-S. Yang, Y.-B. Huang, and Y.-X. Tang. 2012. The R2R3-MYB Transcription Factor Gene Family in Maize K. Wu [ed.],. *PLoS ONE* 7: e37463.

El Karoui, M., M. Hoyos-Flight, and L. Fletcher. 2019. Future Trends in Synthetic Biology—A Report. *Frontiers in Bioengineering and Biotechnology* 7: 175.

Elowitz, M. B., and S. Leibler. 2000. A synthetic oscillatory network of transcriptional regulators. *Nature* 403: 335–338.

Enstone, D. E., C. A. Peterson, and F. Ma. 2002. Root Endodermis and Exodermis: Structure, Function, and Responses to the Environment. *Journal of Plant Growth Regulation* 21: 335–351.

Fernández-Piñán, S. Boher, P. Soler, M. et al. 2021. Transcriptomic analysis of cork during seasonal growth highlights regulatory and developmental processes from phellogen to phellem formation. *Scientific Reports* 11(1).

Fitter, A. H. 2002. Rapid Changes in Flowering Time in British Plants. *Science* 296: 1689–1691.

Fussenegger, M., R. P. Morris, C. Fux, M. Rimann, B. von Stockar, C. J. Thompson, and J. E. Bailey. 2000. Streptogramin-based gene regulation systems for mammalian cells. *Nature Biotechnology* 18: 1203–1208.

Gardner, T. S., C. R. Cantor, and J. J. Collins. 2000. Construction of a genetic toggle switch in Escherichia coli. *Nature* 403: 339–342.

Girard, A-L. Mounet, F. Lemaire-Chamley, M. et al. 2012. Tomato GDSL1 is required for cutin deposition in the fruit cuticle. *Plant Cell* 24(7): 3119-3134.

Gonzales, M. F., T. Brooks, S. U. Pukatzki, and D. Provenzano. 2013. Rapid Protocol for Preparation of Electrocompetent Escherichia coli and Vibrio cholerae. *Journal of Visualized Experiments : JoVE*: 50684.

Gossen, M., and H. Bujard. 1992. Tight control of gene expression in mammalian cells by tetracycline-responsive promoters. *Proceedings of the National Academy of Sciences of the United States of America* 89: 5547–5551.

Gou, J.-Y., X.-H. Yu, and C.-J. Liu. 2009. A hydroxycinnamoyltransferase responsible for synthesizing suberin aromatics in Arabidopsis. *Proceedings of the National Academy of Sciences* 106: 18855–18860.

Gou, M., G. Hou, H. Yang, X. Zhang, Y. Cai, G. Kai, and C.-J. Liu. 2017. The MYB107 Transcription Factor Positively Regulates Suberin Biosynthesis. *Plant Physiology* 173: 1045–1058.

Harrington, S. A., A. E. Backhaus, S. Fox, C. Rogers, P. Borrill, C. Uauy, and A. Richardson. 2020. A heat-shock inducible system for flexible gene expression in cereals. *Plant Methods* 16: 137.

Hoang, M. H. T., X. C. Nguyen, K. Lee, Y. S. Kwon, H. T. T. Pham, H. C. Park, D.-J. Yun, et al. 2012. Phosphorylation by AtMPK6 is required for the biological function of AtMYB41 in Arabidopsis. *Biochemical and Biophysical Research Communications* 422: 181–186.

Hose, E., D. T. Clarkson, E. Steudle, L. Schreiber, and W. Hartung. 2001. The exodermis: a variable apoplastic barrier. *Journal of Experimental Botany* 52: 2245–2264.

Inan, G., Q. Zhang, P. Li, Z. Wang, Z. Cao, H. Zhang, C. Zhang, et al. 2004. Salt Cress. A Halophyte and Cryophyte Arabidopsis Relative Model System and Its Applicability to Molecular Genetic Analyses of Growth and Development of Extremophiles. *Plant Physiology* 135: 1718–1737.

Jeong, H.-J., J. Y. Choi, H. Y. Shin, J.-M. Bae, and J. S. Shin. 2014. Seed-specific expression of seven Arabidopsis promoters. *Gene* 553: 17–23.

Kamiya, T., M. Borghi, P. Wang, J. M. C. Danku, L. Kalmbach, P. S. Hosmani, S. Naseer, et al. 2015. The MYB36 transcription factor orchestrates Casparian strip formation. *Proceedings of the National Academy of Sciences* 112: 10533–10538.

Khalil, A. S., and J. J. Collins. 2010a. Synthetic biology: applications come of age. *Nature Reviews Genetics* 11: 367–379.

Khalil, A. S., T. K. Lu, C. J. Bashor, C. L. Ramirez, N. C. Pyenson, J. K. Joung, and J. J. Collins. 2012. A Synthetic Biology Framework for Programming Eukaryotic Transcription Functions. *Cell* 150: 647–658.

Kosma, D. K., I. Molina, J. B. Ohlrogge, and M. Pollard. 2012. Identification of an Arabidopsis Fatty Alcohol:Caffeoyl-Coenzyme A Acyltransferase Required for the Synthesis of Alkyl Hydroxycinnamates in Root Waxes. *Plant Physiology* 160: 237–248.

Kosma, D. K., J. Murmu, F. M. Razeq, P. Santos, R. Bourgault, I. Molina, and O. Rowland. 2014. AtMYB41 activates ectopic suberin synthesis and assembly in multiple plant species and cell types. *The Plant Journal* 80: 216–229.

Krishnamurthy, P., K. Ranathunge, R. Franke, H. S. Prakash, L. Schreiber, and M. K. Mathew. 2009a. The role of root apoplastic transport barriers in salt tolerance of rice (Oryza sativa L.). 16.

Krishnamurthy, P., K. Ranathunge, R. Franke, H. S. Prakash, L. Schreiber, and M. K. Mathew. 2009b. The role of root apoplastic transport barriers in salt tolerance of rice (Oryza sativa L.). 16.

Lashbrooke, J., H. Cohen, D. Levy-Samocha, O. Tzfadia, I. Panizel, V. Zeisler, H. Massalha, et al. 2016. MYB107 and MYB9 Homologs Regulate Suberin Deposition in Angiosperms. *The Plant Cell* 28: 2097–2116.

Latchman, D. S. 1993. Transcription factors: an overview. *International Journal of Experimental Pathology* 74: 417–422.

Legay, S., G. Guerriero, C. André, C. Guignard, E. Cocco, S. Charton, M. Boutry, et al. 2016. MdMyb93 is a regulator of suberin deposition in russeted apple fruit skins. *New Phytologist* 212: 977–991.

Li-Beisson, Y., G. Verdier, L. Xu, and F. Beisson. 2016. Cutin and Suberin Polyesters. eLS, 1–12. John Wiley & Sons, Ltd.

Liberman, L. M., E. E. Sparks, M. A. Moreno-Risueno, J. J. Petricka, and P. N. Benfey. 2015. MYB36 regulates the transition from proliferation to differentiation in the *Arabidopsis* root. *Proceedings of the National Academy of Sciences* 112: 12099–12104.

Líška, D., M. Martinka, J. Kohanová, and A. Lux. 2016a. Asymmetrical development of root endodermis and exodermis in reaction to abiotic stresses. *Annals of Botany* 118: 667–674.

Liu, W. Stewart, C., N. 2015. Plant synthetic biology. *Trends in plant science* 20: 309-317

Luo, X., M. A. Reiter, L. d'Espaux, J. Wong, C. M. Denby, A. Lechner, Y. Zhang, et al. 2019. Complete biosynthesis of cannabinoids and their unnatural analogues in yeast. *Nature* 567: 123–126.

LUX, A., S. MORITA, J. ABE, and K. ITO. 2005. An Improved Method for Clearing and Staining Free-hand Sections and Whole-mount Samples. *Annals of Botany* 96: 989–996.

Ma, N. L., W. A. Che Lah, N. Abd. Kadir, M. Mustaqim, Z. Rahmat, A. Ahmad, S. D. Lam, and M. R. Ismail. 2018. Susceptibility and tolerance of rice crop to salt threat: Physiological and metabolic inspections. *PLoS ONE* 13: e0192732.

Mallikarjuna Swamy, B. P., S. Marundan, M. Samia, R. L. Ordonio, D. B. Rebong, R. Miranda, A. Alibuyog, et al. 2021. Development and characterization of GR2E Golden rice introgression lines. *Scientific Reports* 11: 2496.

Matzke, K., and M. Riederer. 1991. A comparative study into the chemical constitution of cutins and suberins from Picea abies (L.) Karst., Quercus robur L., and Fagus sylvatica L. *Planta* 185: 233–245.

Medford, J. I. and A. Prasad. 2014. Plant synthetic biology takes root. *Science* 346: 162–163.

Medford, J. I., K. Morey, T. Kassaw, and M. Antunes. 2020. Synthetic desalination genetic circuit in plants. U.S. Patent application no. 16/492584.

Meissner, R. C., H. Jin, E. Cominelli, M. Denekamp, A. Fuertes, R. Greco, H. D. Kranz, et al. 1999. Function search in a large transcription factor gene family in Arabidopsis: assessing the potential of reverse genetics to identify insertional mutations in R2R3 MYB genes. *The Plant Cell* 11: 1827–1840.

Millard, P. S., B. B. Kragelund, and M. Burow. 2019. R2R3 MYB Transcription Factors – Functions outside the DNA-Binding Domain. *Trends in Plant Science* 24: 934–946.

Miyashima, S., and K. Nakajima. 2011b. The root endodermis: A hub of developmental signals and nutrient flow. *Plant Signaling & Behavior* 6: 1954–1958.

Molina, I., Y. Li-Beisson, F. Beisson, J. B. Ohlrogge, and M. Pollard. 2009. Identification of an Arabidopsis Feruloyl-Coenzyme A Transferase Required for Suberin Synthesis. *Plant Physiology* 151: 1317–1328.

Molina, I., J. B. Ohlrogge, and M. Pollard. 2008. Deposition and localization of lipid polyester in developing seeds of Brassica napus and Arabidopsis thaliana. *The Plant Journal* 53: 437–449.

Moon, G., B. Clough, C. Peterson, and W. Allaway. 1986. Apoplastic and Symplastic Pathways in Avicennia marina (Forsk.) Vierh. Roots Revealed by Fluorescent Tracer Dyes. *Functional Plant Biology* 13: 637.

Naseer, S., Y. Lee, C. Lapierre, R. Franke, C. Nawrath, and N. Geldner. 2012. Casparian strip diffusion barrier in Arabidopsis is made of a lignin polymer without suberin. *Proceedings of the National Academy of Sciences* 109: 10101–10106.

Oehmke, S. 2020. Design and quantification of a cell type specific genetic circuit in plants. Master's thesis. Colorado State University, Fort Collins, CO.

Oppenheimer, D., G. Herman, P., L. Sivakumaran, S. et al. 1991. A *myb* gene required for leaf trichome differentiation in Arabidopsis is expressed in stipules. *Cell* 67: 483-493.

Osorio, C. E. 2019. The Role of Orange Gene in Carotenoid Accumulation: Manipulating Chromoplasts Toward a Colored Future. *Frontiers in Plant Science* 10.

Pauluzzi, G., F. Divol, J. Puig, E. Guiderdoni, A. Dievart, and C. Périn. 2012. Surfing along the root ground tissue gene network. *Developmental Biology* 365: 14–22.

Philippe, G., I. Sørensen, C. Jiao, X. Sun, Z. Fei, D. S. Domozych, and J. K. Rose. 2020. Cutin and suberin: assembly and origins of specialized lipidic cell wall scaffolds. *Current Opinion in Plant Biology* 55: 11–20.

Pitzschke, A., S. Datta, and H. Persak. 2014. Mitogen-activated protein kinase-regulated AZI1 – an attractive candidate for genetic engineering. *Plant Signaling & Behavior* 9: e27764.

Pollard, M., F. Beisson, Y. Li, and J. B. Ohlrogge. 2008. Building lipid barriers: biosynthesis of cutin and suberin. *Trends in Plant Science* 13: 236–246.

Potrykus, I. 2001. Golden Rice and Beyond. *Plant Physiology* 125: 1157–1161.

Rains, M. K., N. D. Gardiyehewa de Silva, and I. Molina. 2018. Reconstructing the suberin pathway in poplar by chemical and transcriptomic analysis of bark tissues. *Tree Physiology* 38: 340–361.

Ranathunge, K., and L. Schreiber. 2011. Water and solute permeabilities of Arabidopsis roots in relation to the amount and composition of aliphatic suberin. *Journal of Experimental Botany* 62: 1961–1974.

Rawson, H. M., J. E. Begg, and R. G. Woodward. 1977. The effect of atmospheric humidity on photosynthesis, transpiration and water use efficiency of leaves of several plant species. *Planta* 134: 5–10.

Rio, D. C., M. Ares, G. J. Hannon, T. W. Nilsen. 2010. Purification of RNA using TRIzol (TRI reagent). *Cold Spring Harbor Protocols*.

Rivero, L., R. Scholl, N. Holomuzki, D. Crist, E. Grotewold, and J. Brkljacic. 2014. Handling Arabidopsis Plants: Growth, Preservation of Seeds, Transformation, and Genetic Crosses. *In* J. J. Sanchez-Serrano, and J. Salinas [eds.], Arabidopsis Protocols, Methods in Molecular Biology, 3–25. Humana Press, Totowa, NJ.

Ro, D.-K., E. M. Paradise, M. Ouellet, K. J. Fisher, K. L. Newman, J. M. Ndungu, K. A. Ho, et al. 2006. Production of the antimalarial drug precursor artemisinic acid in engineered yeast. *Nature* 440: 940–943.

Robards, A. W., S. M. Jackson, D. T. Clarkson, and J. Sanderson. 1973. The structure of barley roots in relation to the transport of ions into the stele. *Protoplasma* 77: 291–311.

Roppolo, D., B. De Rybel, V. D. Tendon, A. Pfister, J. Alassimone, J. E. M. Vermeer, M. Yamazaki, et al. 2011. A novel protein family mediates Casparian strip formation in the endodermis. *Nature* 473: 380–383.

Schaub, P., F. Wüst, J. Koschmieder, Q. Yu, P. Virk, J. Tohme, and P. Beyer. 2017. Nonenzymatic β-Carotene Degradation in Provitamin A-Biofortified Crop Plants. *Journal of Agricultural and Food Chemistry* 65: 6588–6598.

Schreiber, L. 2010. Transport barriers made of cutin, suberin and associated waxes. *Trends in Plant Science* 15: 546–553.

Schreiber, L., R. Franke, and K. Hartmann. 2005. Wax and suberin development of native and wound periderm of potato (Solanum tuberosum L.) and its relation to peridermal transpiration. *Planta* 220: 520–530.

Schreiber, L., K. Hartmann, and M. Skrabs. 1999. REVIEW ARTICLE Apoplastic barriers in roots: chemical composition of endodermal and hypodermal cell walls.

Shiono, K., M. Ando, S. Nishiuchi, H. Takahashi, K. Watanabe, M. Nakamura, Y. Matsuo, et al. 2014. RCN1/OsABCG5, an ATP-binding cassette (ABC) transporter, is required for hypodermal suberization of roots in rice (Oryza sativa). *The Plant Journal* 80: 40–51.

Shukla, V. Han, J. Cleard, F. et al. 2021. Suberin plasticity to developmental and exogenous cues is regulated by a set of MYB transcription factors. *Proceedings of National Academy of Sciences* 118:39.

Singh, C., and L. Jacobson. 1977. The Radial and Longitudinal Path of Ion Movement in Roots. *Physiologia Plantarum* 41: 59–64.

Stracke, R., M. Werber, and B. Weisshaar. 2001. The R2R3-MYB gene family in Arabidopsis thaliana. *Current Opinion in Plant Biology* 4: 447–456.

To, A., J. Joubès, J. Thueux, S. Kazaz, L. Lepiniec, and S. Baud. 2020. AtMYB92 enhances fatty acid synthesis and suberin deposition in leaves of Nicotiana benthamiana. *The Plant Journal* 103: 660–676.

Toledo-Ortiz, G., E. Huq, and M. Rodriguez-Concepcion. 2010. Direct regulation of phytoene synthase gene expression and carotenoid biosynthesis by phytochrome-interacting factors. *Proceedings of the National Academy of Sciences* 107: 11626–11631.

Tsugama, D., S. Liu, and T. Takano. 2012. Drought-induced activation and rehydration-induced inactivation of MPK6 in Arabidopsis. *Biochemical and Biophysical Research Communications* 426: 626–629.

Vishwanath, S. J., C. Delude, F. Domergue, and O. Rowland. 2015. Suberin: biosynthesis, regulation, and polymer assembly of a protective extracellular barrier. *Plant Cell Reports* 34: 573–586.

Wang, J.-W., A. Wang, K. Li, B. Wang, S. Jin, M. Reiser, and R. F. Lockey. 2015. CRISPR/Cas9 nuclease cleavage combined with Gibson assembly for seamless cloning. *BioTechniques* 58: 161–170.

Xiong, L. Zhu, J. 2002. *The Arabidopsis Book*. Salt Tolerance, 1-22. American Society of Plant Biologists.

Yeats, T., H. Martin, L., B., B. Viart, H., M-F. et al. 2012. The identification of cutin synthase formation of the plant polyester cutin. *Nature Chemical Biology* 8(7):609-611.

Yeats, T., H. Huang, W. Chatterjee, S. et al. 2014. Tomato cutin deficient 1 (CD1) and putative orthologs comprise an ancient family of cutin synthase-like (CUS) proteins that are conserved among land plants. *The Plant Journal* 77(5):667-675.

Zhang, P., R. Wang, X. Yang, Q. Ju, W. Li, S. Lü, L. P. Tran, and J. Xu. 2020. The R2R3-MYB transcription factor ATMYB49 modulates salt tolerance in *Arabidopsis* by modulating the cuticle formation and antioxidant defence. *Plant, Cell & Environment* 43: 1925–1943.

Ziegler, J., S. Schmidt, N. Strehmel, D. Scheel, and S. Abel. 2017. Arabidopsis Transporter ABCG37/PDR9 contributes primarily highly oxygenated Coumarins to Root Exudation. *Scientific Reports* 7: 3704.

A.1 Media preparation protocols

A1.1 Murashige and Skoog (MS) Basal Media

MS media, either solid or liquid, was prepared as follows. Forty grams of sucrose, 17.6g MS Basal Medium (PhytoTech Labs, Lenexa, KS), and 2g MES (Sigma Aldrich, St. Louis, MO) were dissolved in 3200mL deionized water. The solution was then brought to 4000mL via addition of deionized water. The pH of the solution was brought to 5.7 using 1M KOH. After pH verification solution is put in bottles in 500mL aliquots. If solid media is required add 3g Plant Media Phyto Agar to each aliquot. Finally, all aliquots are autoclaved.

A1.2 Luria Broth (LB) Media

LB media, either solid or liquid was prepared as follows. Forty grams tryptone (Gibco, Detroit, MI), 20g yeast extract (Gibco, Detroit, MI), and 40g NaCl were dissolved in 3800mL deionized water. The solution was then brought up to 4000mL via addition of deionized water. The pH of the solution was brought to 7.0 using 3M NaOH. After pH verification the solution is put into bottles in 500mL aliquots. If solid media is required add 7.5g Agar II to each aliquot. Finally, all aliquots are autoclaved.

A1.3 New Infiltration Media (NIM)

NIM was prepared by dissolving 200g sucrose and 0.812g $MgCl_2$ in 3600mL deionized water. The solution was then brought up to 4000mL via addition of deionized water. If using immediately, the solution is ready. If storage is necessary aliquot 500mL into bottles and autoclave solution.

A.2 Primer sequences

Primer number	Primer sequence (5'>3')	Use
1	TAGTAATAATGGGGCGATCACCATG	Generation of MYB9 PCR fragment
2	CAATCTTGTCTATTCAGGAAATGGCC	Generation of MYB9 PCR fragment
3	TGTAATATATAAGTTAGGAAGATGAGAGAGAAG	Generation of MYB67 PCR fragment
4	AGAAAGTGGCAATTATTCATATATATACACT	Generation of MYB67 PCR fragment
5	AGAAGGCTAAGGAATGTCGG	Generation of MYB92 PCR fragment
6	GATCATCTAACATGGGAAGATCTCC	Generation of MYB92 PCR fragment
7	AGAGATAATAAGACAACCTAATCAGAGAGAGATG	Generation of MYB93 PCR fragment
8	TAACTAAGATATAACGTTCATGAGGCTTTCG	Generation of MYB93 PCR fragment
9	CGCAAGTCAAAATGCATTGAGCTTATCT	Sanger sequencing of junction between ABCG37 promoter and MYB genes in NTB constructs
10	ACGAATGGATCCTAGTAATAATGGGG	Addition of BamHI restriction site 5' of MYB9

| 11	ACGAATGGATCCGGAAGATGAGA	Addition of BamHI restriction site 5' of MYB67
12	CAACTCTTTAAGCCAAGCCGATGGGAAGATCTCCTATC	Gibson Assembly of NTB092 construct
13	AACGATCGGGGAAATTCGAGCTAAGGAATGTCGGAAAATATAG	Gibson Assembly of NTB092 construct
14	TCCTTCTTCTGACGCTTTTGATCCTG	Site directed mutagenesis of Ser^{278} to Asp^{278} of MYB67
15	GTGTTAAACAAAATGTCCATG	Site directed mutagenesis of Ser^{278} to Asp^{278} of MYB67
16	TTTGTTTAACGATCCTTCTTCTTCTGC	Site directed mutagenesis of Thr^{274} to Asp^{274} of MYB67
17	ATGTCCATGTTGAGATCATC	Site directed mutagenesis of Thr^{274} to Asp^{274} of MYB67
18	AGTCGGGCTCGGGTCCGAGGATGGCGTG	Site directed mutagenesis of Ser^{305} to Asp^{305} of MYB102
19	CACGCCATCCTCGGACCCGAGCCCGACT	Site directed mutagenesis of Ser^{305} to Asp^{305} of MYB102
20	GGTCTTAAACGATCCATCCTCGAGC	Site directed mutagenesis of Thr^{301} to Asp^{301} of MYB102
21	GAATTTGCGAAGTTGAAG	Site directed mutagenesis of Thr^{301} to Asp^{301} of MYB102
22	TTTGTTAAAGGCCTTGTCTGG	Test for genomic DNA contamination in cDNA synthesis
23	ACTCATCCAGTCTGTGTCC	Test for genomic DNA contamination in cDNA synthesis

24	ACAATATTCAGTCTCAGGTTGC	Test for genomic DNA contamination in cDNA synthesis
25	TTCGGTTAATGGCATTGAG	Test for genomic DNA contamination in cDNA synthesis
26	GACCTTTAACTCTCCCGCTATG	ACT2 qPCR
27	GAGACACACCATCACCAGAAT	ACT2 qPCR
28	CCTTTAGTCTCACCGATCTCAC	KCS2 qPCR
29	GAGGACGAGTTGTGAAGTAGAG	KCS2 qPCR
30	ATGTTCGCTGCCGAGTTT	ABCG6 qPCR
31	CTTCATCTCCGATCACCGTATTC	ABCG6 qPCR
32	CGAGGTTCTCGTTCACTACTATC	FACT qPCR
33	CCACCACTACAACTCCTTCTC	FACT qPCR
34	CCTCTTATCTCTCACTGCTTCAG	GELP51 qPCR
35	TTATTTCCGGCATCGACTAGAG	GELP51 qPCR

A.3 Plasmid maps
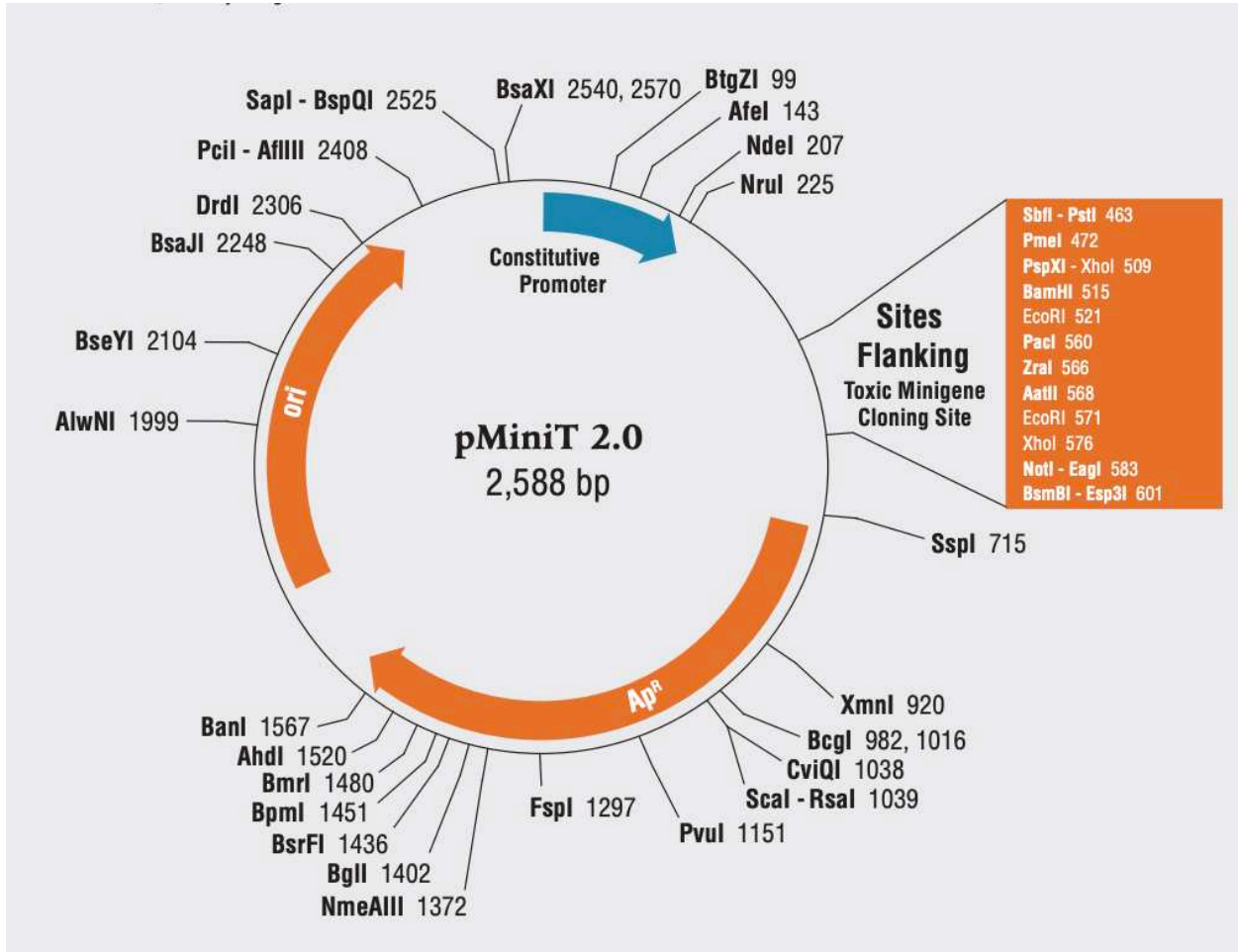
Figure A.3-1 Plasmid map of pMini 2.0 cloning vector. Image reference: New England Biolabs, 'pMiniT 2.0.'
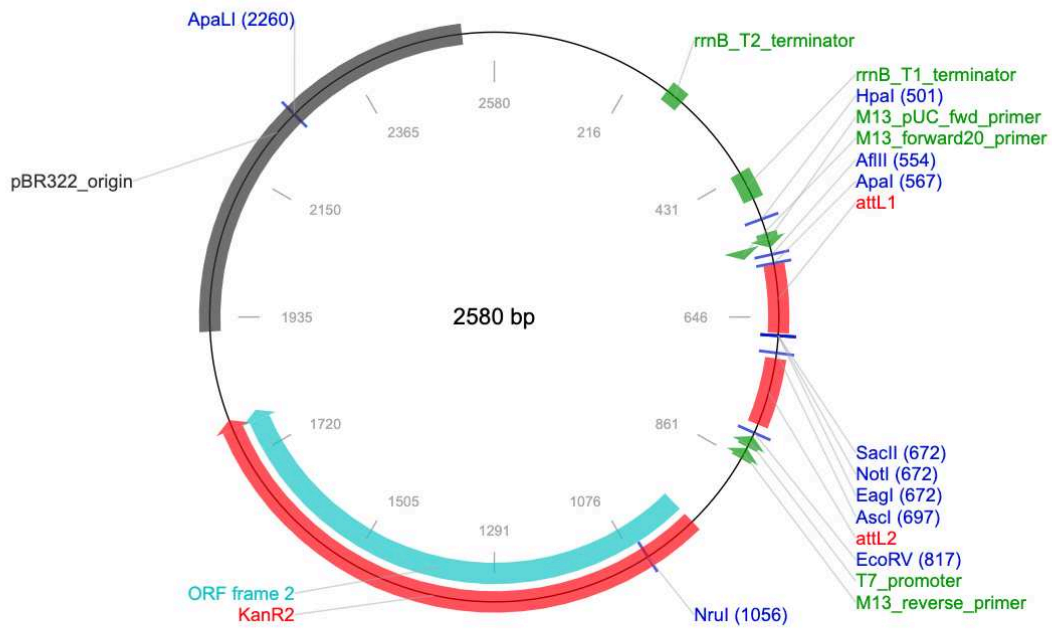
Figure A.3-2 Plasmid map of pENTR/D-TOPO cloning vector. Image reference: Addgene vector database. 'Plasmid: pENTR/SD/D-TOPO.'